

DNA under high tension: Overstretching, undertwisting, and relaxation dynamics

John F. Marko

Department of Physics, The University of Illinois at Chicago, 845 West Taylor Street, Chicago, Illinois 60607

(Received 7 October 1997)

Single-molecule experiments indicate that a double-stranded DNA increases in length if put under tension greater than 10 pN; beyond this point its conformation can no longer be described using an inextensible wormlike-chain model. The simplest extensible wormlike chain with twist rigidity is considered as a model for DNA under tension, and it is found that the fact that DNA is chiral demands that stretching be coupled to twisting at linear order in elastic theory; stretching a DNA is thus a way to perturb its twist degree of freedom. Nonlinearities are essential to stabilize the experimentally observed “overstretched” state which is roughly 1.6 times the length of the unperturbed double helix, and undertwisted. If DNA linkage is held fixed, the transition to the overstretched state is strongly broadened. The overstretching model is also used to study DNA conformational change driven by the binding of RecA proteins to the double helix, and indicates that RecA cannot be dissociated from DNA by application of tension. Finally, relaxation dynamics of a stretched DNA are discussed. The existence of a dynamical writhe instability for a chain without fixed linkage number is demonstrated; it is also argued that the (untwisted) interior of an overstretched DNA will supercoil as it relaxes. [S1063-651X(98)08302-0]

PACS number(s): 87.15.-v, 36.20.Ey, 64.90.+b

I. INTRODUCTION

Single-molecule elasticity measurements have shown that the entropic elasticity of the DNA double helix in aqueous solution is remarkably well described by the wormlike-chain (WLC) model with fixed contour length [1–3] over a wide range of forces. However, recent experiments of Refs. [4] and [5] indicate that if the tension on a DNA exceeds about 10 pN, its contour length increases. At first this change is a small fraction of the DNA length, growing linearly with applied tension, but at about 70 pN the molecule abruptly increases in length by a factor of 1.6 over a few pN increase in force. On the basis of molecular modeling [4,6], it has been suggested that this “overstretched DNA” or “S-DNA” has highly tilted base pairs, and a reduced double-helix diameter.

What are the implications of this remarkable transition? Previously, statistical-mechanical models of DNA elasticity assumed inextensibility [3,7], or did not consider how stretching might interact with bending and twisting [4]. Kamien *et al.* [8] recently found a linear coupling of stretch to twist in several elastic models of DNA; they then analyzed data of Ref. [9] which indicated a lengthening of the double helix caused by undertwisting to extract the twist-stretch coupling constant. Parallel work [10] on an extensible wormlike-chain model for DNA also concluded that there was a linear twist-stretch coupling, and through analysis of the overstretching behavior of twist-constrained DNA [11] found a value of the twist-stretch coupling comparable to that of Kamien *et al.*

These comparable twist-stretch coupling estimates coming from quite different experiments and force regimes suggest that the idea behind the work of both these groups, namely, that the handedness of DNA demands that twisting be coupled to stretching at linear order in elasticity theory, and therefore that a small increase in DNA contour length is accompanied by a proportional untwisting, is reasonable.

This has been further emphasized in recent work of Moroz and Nelson [12], who used the extensible WLC model, including linear extensibility and twist-stretch coupling effects, to study the effect of twisting of DNA on its entropic elasticity for forces < 10 pN, again using experimental data [9] to determine the elastic constants.

In this paper, a more detailed discussion of the extensible WLC model for overstretching of DNA introduced previously [10] is presented. This model quantitatively describes the 70-pN force “plateau” observed by Cluzel *et al.* [4] and Smith *et al.* [5], signifying the transition from *B*-DNA (the biologically relevant conformation of the double helix) to overstretched *S*-DNA (Sec. II). Taking the twist-stretch coupling obtained previously, *S*-DNA is predicted to have a helix repeat of about 12.5 bp (base pairs), about 20% more than the 10.5-bp repeat of *B*-DNA.

In Sec. III, the elasticity of DNA with its twist held fixed is considered, using the approach of Moroz and Nelson [12] and Bouchiat and Mezard [13] to analyze how the bending fluctuations are modified by constraint of the double-helix linkage number. For forces > 10 pN there is an increasing range of σ over which writhing of the double helix is small. This motivates a no-writhe approximation for analysis of the effect of linkage number constraint on overstretching (Sec. III B) [10]. Holding the linkage number fixed (i.e., holding on to both strands of the double helix at both ends) results in a strong broadening of the overstretching transition, as reported by Cluzel [11].

In Sec. IV, the overstretching model is extended to describe the binding of RecA proteins to DNA. RecA catalyzes the initial stages of general recombination in bacteria, by introducing a foreign single strand into a homologous double helix. To do this, RecA is capable of binding three single-stranded DNA's. In test-tube experiments, RecA can form filaments around double-stranded DNA, in the process increasing its helix repeat to about 18 bp and lengthening it by 1.5 times [14].

By combining fields driving untwisting and lengthening with the double helix elasticity, a simple model for RecA bound to double-stranded DNA (RecA-dsDNA) is obtained. The model indicates that the overstretching plateau is abolished by the binding of RecA, and that RecA cannot be dissociated by tension, in the manner of DNA-binding proteins that store length in loops or bends [15]. Calculation of DNA strain and twist near a “domain wall” between RecA-dsDNA and bare double helix shows that there is a region of a few bp in extent over which the twist and stretching relax, corresponding to the correlation length for strain fluctuations. The free energy cost of the domain wall and its structure suggests that RecA monomers are most readily added to RecA-DNA filaments at existing domain walls.

At the end of Sec. IV, the elasticity of internal base-pair tilt is briefly described. At linear order in elasticity, tilt is linearly coupled to the twist and stretching degrees of freedom. In principle, tilt elasticity should be considered in the model of Sec. IV, since DNA base-pair tilt is constrained when bound to RecA. However, the lack of any experimental data indicating the linear elastic constants, combined with the fact that the tilt constraint imposed by RecA is far from the small deformation regime, precludes inclusion of tilt elasticity in the RecA-DNA model.

In Sec. V the relaxation dynamics of highly stretched DNA are considered. Previously it was argued that an over-stretched, and therefore highly undertwisted DNA, if abruptly released, will relax by formation of supercoiled (writhed) domains in its interior [10] and finally by “flowering” at its free end(s) [16]. This was argued to occur because, barring writhing, the twist must exit the free end, and as a result the interior twist will be stable for a long enough time for supercoiling to occur. Over this time window, the interior of the molecule cannot “know” whether the twist on it is due to a static torque, or is supported by hydrodynamic drag. Here it is shown that there is an initial fast relaxation of length with little twist relaxation. Following this initial relaxation, if more than a threshold amount of twist remains in the chain, it will writhe. The dynamics are analyzed without reference to double-helical linkage number [17] which is of course not defined for a linear chain with a free end.

II. CHIRAL EXTENSIBLE WORMLIKE CHAIN

The inextensible WLC is described by the orientation of its tangent $\hat{\mathbf{t}}$ as a function of arc length s ; deformation of the chain away from its straight configuration costs a bending energy per length proportional to an elastic constant times the square of curvature, $k_B T A (d\hat{\mathbf{t}}/ds)^2/2$. The parameter A is the persistence length, or the distance along a freely fluctuating chain over which $\hat{\mathbf{t}}$ is deflected by about 1 rad. Inextensibility of the chain is enforced by the relation $d\mathbf{r}/ds = \hat{\mathbf{t}}$ between the tangent and the position $\mathbf{r}(s)$ of point s along its contour. The WLC with $A \approx 50$ nm describes DNA under tensions less than 10 pN, in ≥ 10 mM univalent salt solution [7].

DNA has twisting elasticity in addition to bending elasticity [18]. Twisting is described by the angle per arc length that the base pairs rotate around $\hat{\mathbf{t}}$; an unperturbed DNA has a helix repeat of 3.5 nm (10.5 base pairs, or bp), and thus a

twist rate of 1.8 rad/nm. Deviations Ω of the twisting away from this rate cost an elastic energy per length of $k_B T C_0 \Omega^2/2$. Here C_0 is the persistence length for twist fluctuations: various experiments indicate $C_0 \approx 75$ nm [18,19] (note, however, the value of 110 nm recently obtained by Moroz and Nelson [12]). The coupling of twisting to bending of DNA may be argued to be negligible under most circumstances [20]; no compelling experimental evidence for coupled twisting and bending elasticity, or a proposed coupling of stretching and bending [8], as yet exists. By contrast, there are observable effects of a linear coupling between stretching and twisting of the double helix [8,12,10].

Experiment indicates that intrinsic stretching elasticity must be added to the WLC [7,21,22]. Arc length s is no longer usable, and must be replaced with an internal coordinate ξ , which may be considered either as arc length in the absence of thermal fluctuations or chemical distance along the chain. Without thermal fluctuations, the chain contour length is supposed to be L_0 . The relation between position and the tangent becomes $d\mathbf{r}/d\xi = v\hat{\mathbf{t}}$, where $v - 1 \equiv u$ is the axial strain. Small extensions can be supposed to cost energy per length $k_B T \gamma u^2/2$.

The internal *tilt* of base pairs, with respect to $\hat{\mathbf{t}}(\xi)$ is another local strain degree of freedom of the double helix. For very short DNAs (tens of bp) under high tension, the tilt, and therefore the elastic free energy, will depend on how tension is applied; i.e., to opposite strands (3′–3′ or 5′–5′ connections) or to the same strand (5′–3′ connections). Dependence of elasticity on connections made to the molecule has been observed in numerical simulations of 12-bp molecules [6]. In this section tilt is not explicitly considered as long chains (50 kb) are under discussion, for which base-pair tilt far from the chain ends will settle into an equilibrium independent of boundary conditions. This occurs because tension couples only to base-pair tilt *at* the chain ends, while it is coupled to the tangent and stretch degrees of freedom along the entire chain length (double helix twist, also an “internal” degree of freedom, is introduced here because external torques, which couple to twist along the entire chain contour, will be discussed in Sec. III).

To describe a long, chiral extensible WLC with twist rigidity subject to a tension > 10 pN applied to its ends, three strain variables need be considered. These are the rate of change of tangent, twist angle, and extension, $d\hat{\mathbf{t}}/d\xi$, Ω , and u , each of which is zero for an unperturbed double helix. The square of each of these quantities is a term in the elastic energy. At scales large compared to the helix repeat, no linear twist-bend coupling occurs as no quadratic rotationally invariant object can be formed from $d\hat{\mathbf{t}}/d\xi$ and Ω ; similarly, there cannot be a quadratic term coupling u to $d\hat{\mathbf{t}}/d\xi$ (note that at small scales comparable to the helix repeat the anisotropy of the double helix leads to an elasticity theory that includes twist-bend [20] and stretch-bend [8] couplings, but their effects on the large scales of interest here are higher-than-linear-order contributions to the effective elastic theory for bending, twisting, and stretching, see Ref. [20]).

A linear coupling of twist to stretching, or a Ωu term is allowed: sign reversal of neither u nor Ω is a symmetry, the former because stretching and compression are distinct, and the latter because DNA is chiral, making overtwisting and

undertwisting distinct. As long as $g^2 < C_0 \gamma_0$, this term does not destabilize the unstressed state ($\Omega = u = 0$), and must be included; it describes how untwisting the double helix lengthens it, as the sugar-phosphate backbones are straightened. This simple picture suggests $g > 0$ [8].

Therefore, DNA should be described by an elastic energy of the form

$$\frac{E}{k_B T} = \int_0^{L_0} d\xi \left[\frac{A}{2} \left(v \frac{d\hat{\mathbf{t}}}{d\xi} \right)^2 + \frac{C_0}{2} \Omega^2 + \frac{\gamma_0}{2} u^2 + g u \Omega + \frac{w}{2} \left(\frac{du}{d\xi} \right)^2 + V(u) - \frac{f}{k_B T} v \hat{\mathbf{t}} \cdot \hat{\mathbf{z}} \right]. \quad (1)$$

In addition to the linear elastic terms described above, a $(du/d\xi)^2$ term is included to introduce a correlation length for $u(s)$, and a general potential $V(u)$ is added to define a stable ‘‘overstretched’’ state.

Large strains are stereochemically limited, leading $V(u)$ to diverge for sufficiently large $u \approx 0.9$ (the interesting topic of breakage of the double helix is not discussed here). Compressions ($u < 0$) are also limited by hard-core repulsion. For simplicity, these two effects are combined in this paper using the constraint $|u| \leq \alpha$ or equivalently, $V(u) = \infty$ for $|u| \geq \alpha$. Since this paper is concerned with stretching, the precise value of the compression limit plays no role here; addition of an independent limit on compression, or more detailed models of the divergences in V , is straightforward.

The bending energy has had some nonlinear terms added to it to ease computation of the partition function for (1), using standard path integral techniques [21] for the quantum mechanics of a particle in spherical coordinates. The measure used for the $\hat{\mathbf{t}}$ and u fluctuations is $d^3 r[s]$, or equivalently $v^2 du d^2 t$.

The final term of Eq. (1) couples external tension $f \hat{\mathbf{z}}$ to total extension $\mathbf{r}(L_0) - \mathbf{r}(0)$. The twist elastic constant is called C_0 , since it slightly differs from the more commonly used [18] effective twist elasticity constant for the ensemble where u is free to fluctuate, $C = C_0 - g^2/\gamma_0$. Equation (1) is a simple model for any semiflexible polymer with twist rigidity and a chiral structure (e.g., actin filaments, or coiled-coil proteins).

DNAs under tension often have no constraint on their twist, for example when attachments are made via single chemical bonds about which the molecule may freely swivel. In this case, the Ω fluctuations of Eq. (1) may be summed over (using measure $d\Omega[s]$) to yield the effective energy

$$\frac{E}{k_B T} = \int_0^{L_0} d\xi \left[\frac{A}{2} \left(v \frac{d\hat{\mathbf{t}}}{d\xi} \right)^2 + \frac{w}{2} \left(\frac{du}{d\xi} \right)^2 + \frac{\gamma}{2} u^2 + V(u) - \frac{f}{k_B T} v \hat{\mathbf{t}} \cdot \hat{\mathbf{z}} \right], \quad (2)$$

where $\gamma = \gamma_0 - g^2/C_0$; twist fluctuations soften the stretching elasticity. The average twist is

$$\langle \Omega(s) \rangle = -(g/C_0) u(s) \quad (3)$$

thanks to the locality of the twist free energy. If a DNA is stretched, its twist is changed proportionally.

A. Gaussian approximation for freely fluctuating twist

If $u \ll 1$ and $\hat{\mathbf{t}} \cdot \hat{\mathbf{z}} \approx 1$, as is the case for tensions $f \approx 10$ pN, one may retain only terms quadratic in the fluctuation of u , and in the transverse part of $\hat{\mathbf{t}}$, $\mathbf{t}_\perp \equiv \hat{\mathbf{t}} - (\hat{\mathbf{z}} \cdot \hat{\mathbf{t}}) \hat{\mathbf{z}}$:

$$\frac{E}{k_B T} = \int_0^{L_0} d\xi \left[\frac{A}{2} \left(\frac{d\mathbf{t}_\perp}{d\xi} \right)^2 + \frac{w}{2} \left(\frac{du}{d\xi} \right)^2 + \frac{\gamma}{2} \left(u - \frac{f}{k_B T \gamma} \right)^2 + \frac{f}{k_B T} \mathbf{t}_\perp^2 \right]. \quad (4)$$

Here V will be supposed to behave as u^3 for small u , so that it will not play a role in the harmonic length fluctuations.

The Gaussian fluctuations of Eq. (4) may be integrated to find approximate averages of u and \mathbf{t}_\perp^2 , and of the end-to-end extension $z \equiv \langle \mathbf{r}(L_0) - \mathbf{r}(0) \rangle \cdot \hat{\mathbf{z}}$:

$$\langle u \rangle = \frac{f}{k_B T \gamma},$$

$$\langle \Omega \rangle = -\frac{g}{C_0} \frac{f}{k_B T \gamma}, \quad (5)$$

$$\langle \mathbf{t}_\perp^2 \rangle = 2 \int_{-\infty}^{+\infty} \frac{dq}{2\pi(Aq^2 + f/k_B T)} = \left(\frac{k_B T}{A f} \right)^{1/2},$$

$$\frac{\langle z \rangle}{L_0} = 1 + \langle u \rangle - \frac{1}{2} \langle \mathbf{t}_\perp^2 \rangle = 1 - \left(\frac{k_B T}{4A f} \right)^{1/2} + \frac{f}{k_B T \gamma}.$$

The final line of Eq. (5) was obtained previously [7,22]; measurements on freely swiveling molecules find $\gamma \approx 300$ nm⁻¹ [4,5,23].

B. Overstretching with freely fluctuating twist

For large forces ≈ 40 pN, $\langle u \rangle$ is no longer small, and experimentally it is seen that at a force of 70 pN, z/L changes from about 1.1 to 1.6, over only a few pN. This effect can only be accounted for with the nonlinear elasticity $V(u)$ and the domain wall term $(du/d\xi)^2$. Here only the essential terms needed to generate the observed plateau are included: $V(u) = -qu^3/3$ will be assumed which, in concert with constraint $u \leq \alpha$, provides a barrier over which u must pass to reach the overstretched state (recall that the compression is limited to $u > -\alpha$; the results for stretching are not sensitive to this lower limit on u). For unconstrained twist, this model always has $\langle \Omega \rangle = -(g/C_0) \langle u \rangle$, even for large $\langle u \rangle$ (this would be altered by other terms nonlinear in Ω).

The remaining fluctuations in Eq. (2) may be treated exactly by conversion of the statistical path integral to a Schrödinger-like equation for the distribution ψ of $\hat{\mathbf{t}}$ and u [21]. First, consider how ψ at $\xi = 0$ and $\xi = L_0$ are related:

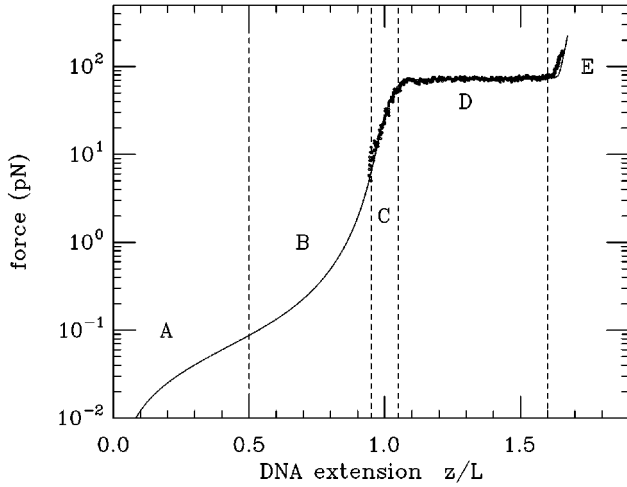


FIG. 1. Elasticity of DNA without twist constraint. (A) For forces less than $k_B T/A \approx 0.1$ pN, random-walk fluctuations are being suppressed; (B) for forces between 0.1 and 10 pN the small curvature fluctuations reduce the length of the DNA by a fraction $\approx (k_B T/Af)^{1/2}$; (C) for forces between 10 and 60 pN, simple linear elasticity of DNA is observed, as the double helix starts to be lengthened; (D) at about 65 pN, a force “plateau” is observed, corresponding to “coexisting” regions of normal and overstretched DNA; (E) finally, above 70 pN, DNA is entirely converted to its overstretched form. Points are experimental results of Cluzel *et al.* for the overstretching transition.

$$\psi(\hat{\mathbf{t}}, u, L_0) = \int d^2 t' du' \int \mathcal{D}\hat{\mathbf{t}} Du e^{-E/k_B T} \psi(\hat{\mathbf{t}}', u', 0), \quad (6)$$

where the energy E is that of Eq. (2). Taking the limit $L_0 \rightarrow 0$ gives a Schrödinger-like equation for the evolution of ψ over a short distance along the chain:

$$\frac{\partial \psi}{\partial \xi} = \left[\frac{1}{2Av^2} \nabla_{\hat{\mathbf{t}}}^2 + \frac{1}{2w} \frac{\partial^2}{\partial u^2} - \frac{\gamma}{2} u^2 - V(u) + \frac{f}{k_B T} v \hat{\mathbf{t}} \cdot \hat{\mathbf{z}} \right] \psi. \quad (7)$$

The stationary states of Eq. (7) satisfy the eigenvalue equation $\partial \psi / \partial s = \lambda \psi$. Finally, the largest λ gives the partition function Z for the entire chain via $\ln Z = k_B T \lambda L_0$. The end-to-end z extension follows as $z/L_0 = k_B T d\lambda/df$.

Since the overstretching transition occurs for high forces, where the width of the $\hat{\mathbf{t}} \cdot \hat{\mathbf{z}}$ distribution is small, it is reasonable to compute λ using the variational “wavefunction”,

$$\psi(\hat{\mathbf{t}}, u) = \frac{1}{\mathcal{N}} \exp[a_0 \hat{\mathbf{t}} \cdot \hat{\mathbf{z}}], \sum_k a_k \sin\left[\frac{\pi k}{2} \left(1 + \frac{u}{\alpha}\right)\right], \quad (8)$$

where $k = 1, 2, 3, \dots$, and where $\mathcal{N} = \int d^2 t du \psi^2$. At the hard limits on extension and compression, $u = \pm \alpha$, the wave function is forced to vanish, but otherwise the u fluctuations are arbitrary. The tangent fluctuations are polarized along the $+z$ axis; this description of the tangent fluctuations was shown to be a good approximation for the inextensible WLC [7].

Given a_k 's, the variational estimate for λ is

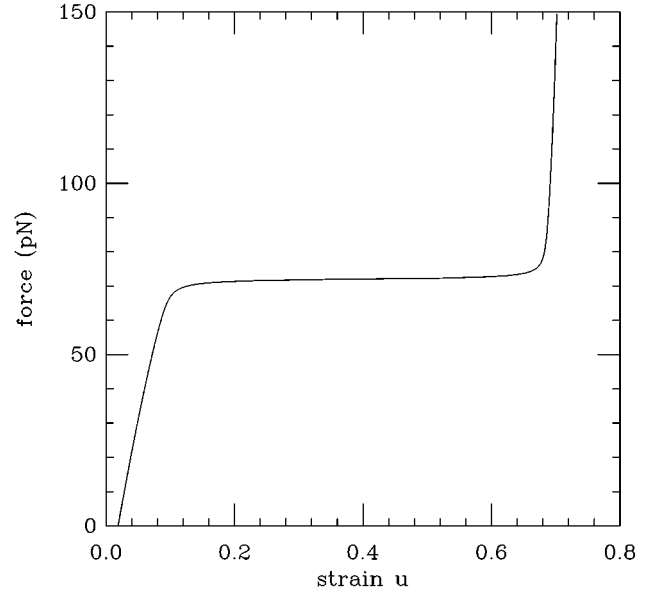


FIG. 2. Dimensionless strain u as a function of applied force. At zero force, the asymmetry in the u potential causes $\langle u \rangle \approx 0.018$. For small forces < 50 pN, u increases linearly with force; at 65 pN, u goes through the overstretching transition; for $f > 80$ pN, u starts to be crushed against its maximum allowed value $\alpha = 0.83$.

$$\lambda = \int d^2 t du \left\{ -\frac{1}{2Av^2} (\nabla_{\hat{\mathbf{t}}} \psi)^2 - \frac{1}{2w} \left(\frac{\partial \psi}{\partial u} \right)^2 + \left[\frac{\gamma}{2} u^2 + V(u) - \frac{f}{k_B T} v \hat{\mathbf{t}} \cdot \hat{\mathbf{z}} \right] \psi^2 \right\}. \quad (9)$$

The free energy is obtained by maximization of λ over the a_k 's (note that for $k = 1, 2, \dots$, this amounts to solution of an eigenvalue equation, the maximum eigenvalue of which can then be maximized with respect to a_0). Convergence occurred when k was cut off at 40.

The result for Eq. (7) for freely fluctuating twists, $A = 50$ nm, $\gamma = 300$ nm $^{-1}$, $q = 560$ nm $^{-1}$, $w = 10$ nm, and $\alpha = 0.83$, is shown in Fig. 1 (note $1 k_B T/\text{nm} = 4.1$ pN at $T = 300$ K). The parameters have been chosen to obtain agreement with both the entropic elasticity data of Ref. [1] (see Ref. [7]) and the *B*-DNA to *S*-DNA transition data of Ref. [4] (solid points in Fig. 1; see also Ref. [10]). The constants γ , q , and w tune the level and the width of the *B*-*S* transition “plateau:” a larger w gives too flat a plateau; larger values of γ give too steep a linear stress-strain behavior for forces slightly below the plateau; changing q alters the force on the plateau. Agreement between experiment and theory above the plateau could easily be improved by addition of additional nonlinear terms to $V(u)$; a more complete model might use a smoothly diverging V with a limit $\alpha \approx 1.1$, to be consistent with the maximum strain $\alpha = 1.14$ observed in “molecular combing” experiments [24] and simulations of extremely extended DNA's [4,6,25] (this large strain is believed to be obtained by a conformational change in the sugars along the backbone, see Ref. [25]). Of course, an independent compression limit would have to be introduced to ensure $v > 0$.

Figure 2 shows how $\langle u \rangle \propto \langle \Omega \rangle$ varies. At zero force, the asymmetry in the u potential leads to $\langle u \rangle_{f=0} = 0.0187$; the

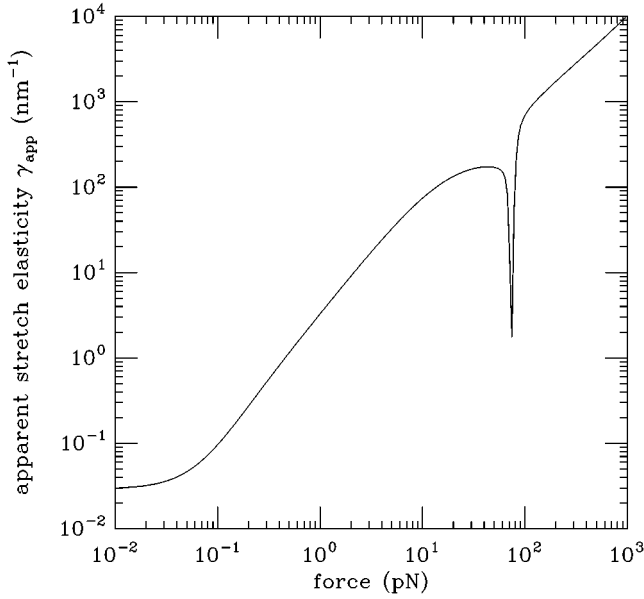


FIG. 3. Apparent stretching elastic constant γ_{app} , defined as the derivative of force with extension, divided by $k_B T$. Note that shortly before the B -DNA to S -DNA transition (downward spike), $\gamma_{app} \approx 180 \text{ nm}^{-1}$; this is significantly below the stretching constant $\gamma = 300$ in the model, thanks to nonlinearities in the overstretching potential.

mean contour length of the chain is slightly increased to $L = L_0(1 + \langle u \rangle)$. Therefore for nonzero g the equilibrium twist is slightly shifted to $\langle \Omega \rangle_{f=0} < 0$.

The undertwisting of S -DNA can be estimated using $\langle \Omega \rangle = -g \langle u \rangle / C_0$. S -DNA has $u \approx 0.7$, and using $g = 30$ (see Sec. III and Ref. [10] where $g = 30$ is obtained; for a determination of $g = 22$, see Ref. [8]; for yet another determination of $g = 26$, see Ref. [12]) and $C_0 = 75 \text{ nm}$, one obtains $\Omega = -0.28 \text{ rad/nm}$. The B state has a twist of about 1.85 rad/nm (a helix repeat of 10.5 bp); the overstretched state is therefore predicted to have a twist of about 1.57 rad/nm (keep in mind that the length ξ is measured along the original B -DNA), or a helix repeat of 12.5 bp . In this model, overstretched DNA is 20% undertwisted with respect to B -DNA. At very high extensions ($z/L_0 \approx 2$), simulations of DNA oligomers indicate that it is possible for *all* the twist to be expelled [25], although this appears to depend on which strands the tension is applied to [6]. Twist of S -DNA needs to be experimentally measured, perhaps by counting the number of turns of a bead that the end of a DNA is attached to during overstretching.

Figure 3 shows the apparent stretching elastic constant for the model, $\gamma_{app} = d(f/k_B T)/d(z/L)$. For the Gaussian approximation to the model, Eq. (5), note that $\gamma_{app} \rightarrow \gamma$ for large forces; fits to this limit have been the strategy for measurement of γ [5,4,23]. For the model including nonlinearities, γ_{app} starts out at low forces at $3/(2A) = 0.03 \text{ nm}^{-1}$ characteristic of random-coil entropic elasticity. As the bending fluctuations are quenched, γ_{app} rises, and finally stabilizes at $\approx 180 \text{ nm}^{-1}$ for forces of $30\text{--}60 \text{ pN}$. Note that γ_{app} plateaus well below the parameter $\gamma = 300 \text{ nm}^{-1}$; this softening is due to the qu^3 term which generates the S -DNA state.

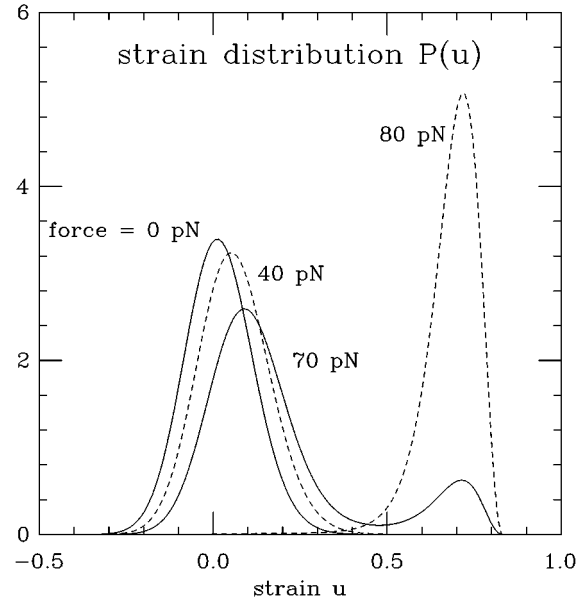


FIG. 4. Probability distribution of stretching strain $P(u)$ for various forces. For zero force the distribution is nearly Gaussian and centered near $u = 0$; as force is increased to 40 pN , the distribution shifts to positive u . On the force plateau (70 pN) the distribution is bimodal, reflecting the coexistence of B -DNA and S -DNA domains; finally, above the plateau (80 pN) $P(u)$ is unimodal, and starts to appear “crushed” by the constraint $u \leq \alpha$.

For forces slightly larger than 60 pN , one encounters the force plateau, and γ_{app} plunges to near zero. Beyond the force plateau, γ_{app} increases rapidly, goes through a “knee” at $f \approx 100 \text{ pN}$, and finally increases approximately linearly with f . This final increase comes from simultaneous quenching of the strain u against its limit α , and the tangent vector $\hat{\mathbf{t}}$ against $\hat{\mathbf{z}}$. A qualitatively similar increase of γ_{app} should occur for real DNA, with the caveats that some stretching of the backbone sugars is expected to occur [25] [recall that this allows extension to $z/L_0 \approx 2.1$; such effects could be built into a more detailed $V(u)$], and that at a force scale $\approx eV/A \approx 1000 \text{ pN}$ the applied force can rupture chemical bonds along the backbone. Ultrahigh-force elasticity of DNA 14-mers has recently been studied using atomic force microscopy techniques [26], and a roughly sevenfold increase in stretching modulus was observed before the DNA broke.

Another way to display the fluctuations in the model is the strain probability distribution $P(u)$, shown in Fig. 4 for various applied forces. This distribution is just $P(u) = \int d^2 t \psi^2(\hat{\mathbf{t}}, u)$. For zero force (leftmost solid curve), the distribution of u is roughly Gaussian with a half-width of 0.1 . This is consistent with the Gaussian limit of Eq. (2) for $w = 10 \text{ nm}$ and $\gamma = 300 \text{ nm}^{-1}$, for which $\langle u^2 \rangle = (4w\gamma)^{-1/2} \approx 0.01$. So, even with zero applied force, there are appreciable “breathing” fluctuations inside B -DNA, with typical local strains of $|u| \approx 0.1$.

The Gaussian approximation indicates that the correlation length for the u fluctuations is $(w/\gamma)^{1/2} \approx 0.2 \text{ nm}$, essentially the spacing of successive base pairs along the double helix. The microscopic picture indicated by this model is thus localized fluctuations on top of a well-defined B -DNA state. Note that some of the plateau slope may be due to the se-

quence inhomogeneity along the DNA which may cause the overstretching transition to occur inhomogeneously. This interesting question has yet to be investigated, either theoretically (through introduction of disorder into, e.g., γ and w), or experimentally (by study of DNA's with different base compositions).

III. HIGHLY EXTENDED DNA WITH FIXED DOUBLE-HELIX LINKAGE

If a DNA is not allowed to freely untwist as it is stretched, its elasticity will be affected. If its ends cannot swivel, the two strands of the DNA have fixed linkage number Lk [9,27,28]. This constraint can be imposed using the relation

$$Lk = Tw + Wr,$$

$$Tw = \frac{\omega_0 L_0}{2\pi} + \frac{1}{2\pi} \int_0^{L_0} d\xi \Omega(\xi), \quad (10)$$

$$Wr = \frac{1}{4\pi} \int_0^L ds \int_0^L ds' \frac{\hat{\mathbf{t}}(s) \times \hat{\mathbf{t}}(s') \cdot [\mathbf{r}(s) - \mathbf{r}(s')]}{|\mathbf{r}(s) - \mathbf{r}(s')|^3},$$

where the coordinate s is arc length along the chain; note that $ds/d\xi = v$ and that s runs from 0 to L as ξ runs from 0 to L_0 .

The nonlocality of the writhe makes exact treatment of fixed linkage difficult in general, and previously [10] this model was treated in the case where $Wr = 0$ was assumed. Recently Moroz and Nelson [12] and Bouchiat and Mezard [13] developed a method for treating the case where the linkage is fixed, which is accurate as long as the tangent vector is near to the $+z$ axis, i.e., as long as the stretching force is sufficiently high (the precise criterion for accuracy of the method is complicated by its reliance on force to keep the molecule from passing through itself; see Ref. [28]). Below this method is used in simplified form, mainly to justify where $Wr = 0$ may be assumed, and to display the linear writhe instability recently discussed Ref. [29], which will play a role in Sec. V.

The writhe may be expressed as an integral of a local function of $\hat{\mathbf{t}}$ using the fact that the writhe modulus 1 is the signed area swept out by $\hat{\mathbf{t}}$ on the unit sphere, divided by 2π [30]. For high extensions, where $\hat{\mathbf{t}} \cdot \hat{\mathbf{z}} \approx 1$, this can be expressed in terms of the usual spherical angles (θ, ϕ) for the orientation of $\hat{\mathbf{t}}$ with respect to the $+z$ axis [27]:

$$Wr = \int_0^L \frac{ds}{2\pi} (1 - \cos\theta) \partial_s \phi = \int_0^{L_0} \frac{d\xi}{2\pi} \frac{\hat{\mathbf{z}} \cdot \hat{\mathbf{t}} \times \partial_\xi \hat{\mathbf{t}}}{1 + \hat{\mathbf{z}} \cdot \hat{\mathbf{t}}}. \quad (11)$$

As long as $\hat{\mathbf{t}}$ stays in the hemisphere where $\hat{\mathbf{t}} \cdot \hat{\mathbf{z}} > 0$, continuity with the state $\hat{\mathbf{t}} = \hat{\mathbf{z}}$ indicates that Eq. (11) is the writhe with no integer offset.

An unperturbed DNA has linkage $Lk_0 = \omega_0 L_0 / 2\pi$, and it is useful to introduce the excess linkage as a fraction of Lk_0 : $\sigma \equiv Lk / Lk_0 - 1$. So, the total twist is

$$\bar{\Omega} = \int_0^{L_0} \frac{d\xi}{L_0} \Omega = \omega_0 \sigma - 2\pi Wr / L_0. \quad (12)$$

This equation constrains $\bar{\Omega}$, which is the zero-wave-number component of $\Omega(\xi)$. We next divide $\Omega = \bar{\Omega} + \delta$, and $u = \bar{u} + \Delta$, where the fluctuations $\delta(\xi)$ and $\Delta(\xi)$ integrate to zero. After integration over δ , the energy is

$$\begin{aligned} \frac{E}{k_B T} = & \int_0^{L_0} d\xi \left[\frac{A}{2} \left(v \frac{d\hat{\mathbf{t}}}{d\xi} \right)^2 + \frac{w}{2} \left(\frac{d\Delta}{d\xi} \right)^2 + \frac{\gamma}{2} \Delta^2 + V(u) \right. \\ & \left. - \frac{f}{k_B T} v \hat{\mathbf{t}} \cdot \hat{\mathbf{z}} \right] + L_0 \left[\frac{C_0}{2} \bar{\Omega}^2 + \frac{\gamma_0}{2} \bar{u}^2 + g \bar{\Omega} \bar{u} - \frac{f}{k_B T} \right]. \end{aligned} \quad (13)$$

A. Gaussian approximation for extension and tangent fluctuations

Dropping the nonlinear potential $V(u)$, and keeping contributions to Eq. (13) through quadratic order in the transverse tangent vector and Δ , and integrating $\Delta(s)$, leads to

$$\begin{aligned} \frac{E}{k_B T} = & \int_0^{L_0} d\xi \left\{ \frac{A}{2} \left(\frac{d\mathbf{t}_\perp}{d\xi} \right)^2 + \frac{f}{2k_B T} \mathbf{t}_\perp^2 \right. \\ & \left. - \frac{1}{2} (C_0 \omega_0 \sigma + g \bar{u}) \hat{\mathbf{z}} \cdot \mathbf{t}_\perp \times \partial_\xi \mathbf{t}_\perp \right\} \\ & + L_0 \left[\frac{C_0}{2} \omega_0^2 \sigma^2 + \frac{\gamma_0}{2} \bar{u}^2 - \left(\frac{f}{k_B T} - g \omega_0 \sigma \right) \bar{u} - \frac{f}{k_B T} \right]. \end{aligned} \quad (14)$$

The equilibrium value of \bar{u} is

$$\langle \bar{u} \rangle = \frac{1}{\gamma_0} \left[\frac{f}{k_B T} - g \left(\sigma \omega_0 - \frac{1}{2} \langle \hat{\mathbf{z}} \cdot \mathbf{t}_\perp \times \partial_\xi \mathbf{t}_\perp \rangle \right) \right], \quad (15)$$

and after integration over \bar{u} the effective energy quadratic in \mathbf{t}_\perp is

$$\begin{aligned} \frac{E}{k_B T} = & \int_0^{L_0} d\xi \left\{ \frac{A}{2} \left(\frac{d\mathbf{t}_\perp}{d\xi} \right)^2 + \frac{f}{2k_B T} \mathbf{t}_\perp^2 \right. \\ & \left. - \frac{1}{2} \left(C \omega_0 \sigma + \frac{gf}{k_B T \gamma_0} \right) \hat{\mathbf{z}} \cdot \mathbf{t}_\perp \times \partial_\xi \mathbf{t}_\perp \right\} \\ & + L_0 \left[\frac{C_0}{2} \omega_0^2 \sigma^2 - \frac{1}{2\gamma_0} \left(\frac{f}{k_B T} - g \omega_0 \sigma \right)^2 - \frac{f}{k_B T} \right]. \end{aligned} \quad (16)$$

In terms of Fourier components $\tilde{\mathbf{t}}_\perp(q)$, the fluctuation part of Eq. (16) is

$$\begin{aligned} \frac{\delta E}{k_B T} = & \frac{A}{2} \int \frac{dq}{2\pi} \{ (q^2 + \mu^2) |\tilde{\mathbf{t}}_\perp|^2 + i\nu q (\tilde{t}_x^* \tilde{t}_y - \tilde{t}_y^* \tilde{t}_x) \}, \\ \mu^2 \equiv & \frac{f}{k_B T A}, \end{aligned} \quad (17)$$

$$\nu \equiv \frac{C \sigma \omega_0 + gf / (k_B T \gamma_0)}{A}.$$

As recognized by Fain, Ostlund, and Rudmek [29], Bouchiat and Mezard [13], and Moroz and Nelson [12], the constraint of fixed linkage couples the x and y components of \mathbf{t} , breaking the parity symmetry of the bending energy.

The eigenenergies of the Gaussian \mathbf{t} energy are $(A/2)(q^2 + \mu^2 \pm \nu q)$, indicating that the average of \mathbf{t}_\perp^2 is

$$\begin{aligned} \langle \mathbf{t}_\perp^2 \rangle &= \frac{1}{A} \int_{-\infty}^{+\infty} \frac{dq}{2\pi} \left[\frac{1}{q^2 + \mu^2 + \nu q} + \frac{1}{q^2 - \mu^2 - \nu q} \right] \\ &= \frac{1}{A \sqrt{\mu^2 - \nu^2/4}}. \end{aligned} \quad (18)$$

The average of the triple product (the writhe) works out to be

$$\frac{1}{2} \langle \hat{\mathbf{z}} \cdot \mathbf{t}_\perp \times \partial_\xi \mathbf{t}_\perp \rangle = \frac{2\pi}{L_0} \langle \mathcal{W}_r \rangle = \frac{\nu/4}{A \sqrt{\mu^2 - \nu^2/4}}. \quad (19)$$

As in Eq. (5), Eq. (18) is combined with Eq. (15) to obtain the extension

$$\begin{aligned} \frac{\langle z \rangle}{L_0} &= 1 + \frac{f}{k_B T \gamma_0} - \frac{g \omega_0 \sigma}{\gamma_0} - \left(\frac{k_B T}{4A f} \right)^{1/2} \\ &\quad \times \left(1 - \frac{g C \sigma \omega_0 + g^2 f / [k_B T \gamma_0]}{2A \gamma_0} \right) \\ &\quad \times \left[1 - \frac{k_B T}{4A f} \left(C \omega_0 \sigma - \frac{g f}{k_B T \gamma_0} \right)^2 \right]^{-1/2} \\ &= 1 + \frac{f}{k_B T \gamma_0} - \frac{g \omega_0 \sigma}{\gamma_0} - \left(\frac{k_B T}{4A f} \right)^{1/2} \\ &\quad - \frac{1}{2} \left(\frac{k_B T}{4A f} \right)^{3/2} (C \omega_0 \sigma)^2 + \text{small terms}. \end{aligned} \quad (20)$$

The first line of Eq. (20) consists of the stretching and twist-stretch terms reported in Ref. [10], which were derived in a different ensemble from above (a fluctuating-link ensemble with writhe forced to be zero was used). The final term which always reduces extension is due to tangent vector fluctuations, and is the central result of Moroz and Nelson [12].

The tangent fluctuation term on the first line of Eq. (20) combines the usual WLC fluctuations with the chiral interaction introduced by the fixed-link condition. The writhe fluctuations are only important when $fA/k_B T < (C \omega_0 \sigma)^2/4$; for larger forces than this, the fluctuations are controlled by the force rather than by linkage. So, for $fA/k_B T \gg (C \omega_0 \sigma)^2/4$, the zero-writhe approximation taken in Ref. [10] is appropriate, at least as long as $\langle u \rangle$ is reasonably small.

On the second line of Eq. (20), the fluctuation term is expanded in powers of $C \omega_0 \sigma$ (this is the dimensionless parameter describing supercoiling [27]), and the first term sensitive to σ is proportional to $f^{-3/2}$. Thus the lowest-order result in an expansion in powers of $1/f^{1/2}$ is just that for the WLC with unconstrained twist [7].

Following Moroz and Nelson, Fig. 5(a) shows Eq. (20) plotted for various forces (0.1, 0.3, 0.6, 0.8, 1.3, 8.0, 20.0, and 50.0 pN, the first six being forces chosen by Strick *et al.*

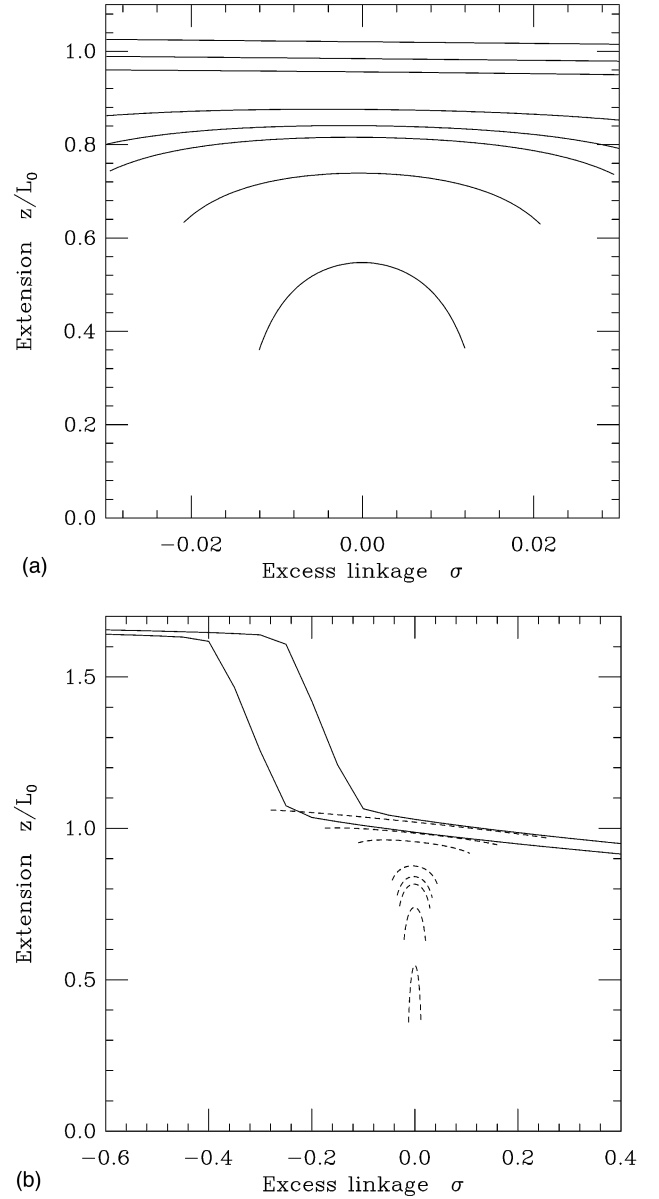


FIG. 5. Extension as a function of specific linkage number, for fixed force. (a) Low- σ regime: curves show an extension as the linkage is varied, for forces of 0.1 (bottom), 0.3, 0.6, 0.8, 1.3, 8.0, 20.0, and 50.0 pN (top), respectively. The curves are computed following the Gaussian calculation of Sec. III A for ≤ 8 pN, and have appreciable curvature indicating length reduction from writhe. (b) Solid curves show overstretching transitions for $f=20$ (lower) and 50 pN (upper), computed in the no-writhe approximation; dashed curves show the results of part (a). As force is increased, the underwinding needed for overstretching is progressively reduced.

in experimental measurements [9]), using the parameters $A = 50$ nm, $\gamma_0 = 310$ nm $^{-1}$, $g = 30$, and $C = 75$ nm (note that Moroz and Nelson [12] have fit experimental data to obtain $C = 110$ nm, while Bouchiat and Mezard find $C \approx 70$ nm in a fit of the same experimental data to numerical results for the inextensible WLC; here the value $C = 75$ nm inferred from studies of supercoiling is used). The curves are plotted in the regime $k_B T (C \omega_0 \sigma)^2 / (4A f) < \frac{1}{2}$, where the tangent vector

fluctuations are reasonably small. By 20 pN, on the σ range of Fig. 5(a), the writhing effects (curvature) are small, but they become visible on the wider range of Fig. 5(b) (dashed curves).

The Gaussian result has an instability at $\nu = \pm 2\mu$, or when $C\omega_0\sigma + gf/(k_B T \gamma_0) = \pm (4Af/k_B T)^{1/2}$. For $g=0$, this is the classical buckling instability of a stiff rod under tension and twist strain [31], recently rederived in Ref. [29]. Beyond this instability, nonlinearities and hard-core self-interactions stabilize plectonemic supercoiling, and extended DNA is found in coexistence with plectonemic supercoils [27,32]. This instability will reappear in Sec. V when dynamics of twisted DNA are discussed.

The free energy [including the nonfluctuation terms from Eq. (16)] can also be computed in the Gaussian approximation,

$$\frac{F}{k_B T L_0} = \frac{1}{A} \left[\frac{Af}{k_B T} - \frac{1}{4} \left(C\omega_0\sigma + \frac{gf}{k_B T \gamma_0} \right)^2 \right]^{1/2} + \frac{C_0}{2} \omega_0^2 \sigma^2 - \frac{f}{k_B T} - \frac{1}{2\gamma_0} \left(\frac{f}{k_B T} - g\omega_0\sigma \right)^2. \quad (21)$$

Again, the writhing instability is evident. For $\sigma=0$, the free energy reduces to that of the WLC under traction in the Gaussian approximation [7].

B. Overstretching of DNA with fixed linkage

Result (20), unlike similar Gaussian results for inextensible WLC's [7] is not the beginning of an asymptotic expansion in powers of $f^{-1/2}$. Although tangent vector fluctuations become progressively smaller as f increases, at the same time the strain u increases, and as the transition to the stretched state is approached, the u fluctuations become progressively larger in amplitude as ‘‘droplets’’ of S -form DNA appear. Finally the chain fully converts to the S form.

A more complete description of the overstretching with fixed linkage could be done using the Schrödinger-like equation technique described above, with the wave function for $\hat{\mathbf{t}}$ expanded in spherical harmonics. This would allow writhing to be accounted for during overstretching. However, since the writhe is small, it is reasonable to assume zero writhe for large forces to study the effect of fixed linkage on the overstretching transition. In this approximation, the total twist, or $\int d\xi \Omega(\xi)$, is fixed.

Fixed $\langle \Omega \rangle$ may be imposed by adding a Lagrange multiplier term $\Gamma \int d\xi \Omega$ to (1); Γ is a torque coupled to the total molecule twist. Integration of Ω results in a linear coupling of Γ to u , and indicates that $\langle \Omega \rangle = -(\Gamma + g\langle u \rangle)/C_0$. So the necessary value of Γ is self-consistently determined. Equivalently, the fixed-twist energy (13) with $\bar{\Omega} = \omega_0\sigma$ can be used with $\langle \bar{u} \rangle$ determined by free energy minimization.

The solid curve of Fig. 6 shows force vs distance with the constraint $\langle \Omega \rangle = \langle \Omega \rangle_{f=\Gamma=0}$ imposed, by computing the Γ necessary to satisfy the constraint, for $g=30$ and $C_0=75$ nm (all other parameters as in Sec. II). Instead of the sharp force plateau seen for the freely fluctuating twist (the dashed line of Fig. 6, the same as the solid curve of Fig. 1), twist constraint causes overstretching to occur as a broad transition over 75–110 pN. This is due to the $g\Gamma u/C_0$ term added to

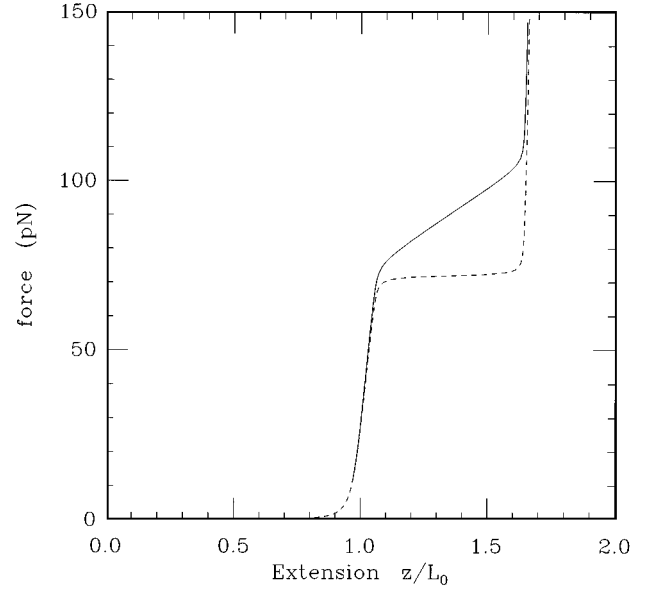


FIG. 6. Overstretching transition with fixed $\sigma=0$ (solid line) compared to the freely fluctuating twist result of Fig. 1 (dashed line). For fixed linkage, the transition plateau is broad, occurring over 70–110 pN.

Eq. (7): as f is increased, Γ increases to keep the twist constant, ‘‘tilting’’ the u potential.

Preliminary data of Ref. [11] indicate that fixing the linkage number modifies DNA elasticity in this way, and the $g=30$ curve of Fig. 6 roughly matches the data. Those data were for a 17 kb $pX\Delta 1$ DNA [11] richer in AT bases (more weakly bound together than GC bases) than the lambda-DNA usually studied [1–5]. An interesting complication is that the AT-rich $pX\Delta 1$ with freely fluctuating twist appears to be described by somewhat smaller γ and w than the $\gamma \approx 300 \text{ nm}^{-1}$ and $w \approx 10 \text{ nm}$ that fit the 47-kb lambda data. Further experimental study of the effect of sequence on elasticity of DNA, with and without constrained twist, is strongly indicated.

The zero-writhe model can also be used to compute extension vs linkage for forces high enough that the writhe is a small fraction of linkage, i.e., roughly for $(C\omega_0\sigma)^2 \ll 4Af/k_B T$. At 50 pN, this condition is $|\sigma| \ll 0.5$. Figure 5(b) shows extension vs linkage over a large linkage range, and it can be seen that for large forces and $\sigma < 0$ there is a transition to S -DNA driven by linkage change (one can alternately state this as a reduction in the force necessary for the transition; for $\sigma \approx -0.1$, the B -DNA to S -DNA transition occurs at ≈ 50 pN). At 20 pN, the transition does not occur until underwindings of $\sigma \approx -0.2$ are reached.

The B -DNA to S -DNA transition thus occurs for progressively less underwinding as forces are increased, and is a first-order-like transition to a state with $\sigma \approx -0.2$ (Sec. II). Under the assumption that S -DNA remains base paired, supported by comparison of the total work needed to create S -DNA [5] to that required to separate and stretch single strands [7] as well as by simulations [6,25], there is a possibility that strand separation, or melting, may be a competing transition. In fact, strand separation has been observed to occur at forces < 5 pN for linkage deficits $\sigma < -0.04$ [27,9]. Thus, at low forces, underwinding leads to strand separation,

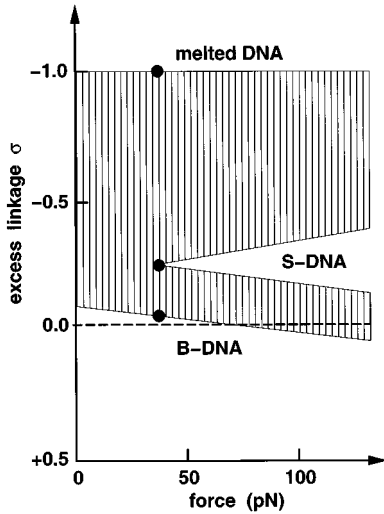


FIG. 7. Conjectured phase diagram for DNA states. Lines indicate “tie lines” between coexisting states with different σ and z/L ; force and torque are nearly constant on the tie lines. First-order-like transitions occur from *B*-DNA to *S*-DNA with increasing force, and from *B*-DNA to melted (strand-separated) DNA for increasing linkage deficit. At some force, *B*-DNA, *S*-DNA, and melted DNA will be in “phase coexistence” on the tie line joining the heavy dots.

i.e., a transition to a state with $\sigma \approx -1$.

Since the *B*-DNA to *S*-DNA transition at large forces involves a different order parameter (double helix twist and shear) than melting (base-pair separation), these phases can have a triple-point phase diagram, as sketched in Fig. 7. This combines the *B*-DNA to *S*-DNA transition observed at 70 pN at $\sigma \approx 0$ [4,5], and according to Fig. 5(b)), at 50 pN for $\sigma = -0.1$, and the melting transitions known to occur at zero and low force. In Fig. 7, force is a thermodynamical variable (like pressure) while σ is an intensive quantity (like density), thus first-order-like transitions are associated with “forbidden” σ regions, spanned by constant-force “tie-lines.” An experiment with unconstrained linkage follows one tie line, generating a force plateau (Fig. 6, dashed line); a measurement at fixed linkage forces coexistence to occur along tie lines of progressively larger force, leading to a broad transition (Fig. 6, solid line). An alternative formulation of this phase diagram would be in terms of force and torque, in which the three first-order-like transition lines would meet at a triple point. It should finally be noted that there is some evidence of first-order-like transitions for *overwound* DNA ($\sigma > 0$) [9].

IV. DEFORMATION OF DNA BY RECA PROTEIN

Is the overstretched state described in the previous sections biologically relevant? It has been suggested [4,12] that overstretched DNA might be similar to the conformation of DNA bound to the protein which accomplishes general recombination in prokaryotes, RecA (note that a homologous protein, Rad51, exists in eukaryotes but does not carry out all the functions of RecA [33]). RecA monomers aggregate to form filaments with a helical structure in a manner vaguely reminiscent of microtubules or actin filaments. The total binding free energy of these filaments including both DNA-RecA and RecA-RecA interactions is roughly $15\text{--}20k_B T$ per

RecA monomer [34]. RecA filaments can bind up to three single strands of DNA, and catalyze recombination of a single strand with a double helix. Finally, it is believed that once a short RecA filament assembles on a double-stranded DNA, it elongates along the double helix.

Once bound to RecA, a double helix has a structure reminiscent of the overstretched DNA. Each RecA monomer binds three base pairs, and the DNA is lengthened by about 1.5 times, undergoing one helical turn only every 18 bp [14]. This suggests that a modification of the model from Sec. II might be used to describe binding of RecA to the double helix. However, it must be noted that molecular modeling suggests that overstretched DNA has highly tilted base pairs [4,25,6], while the bases in RecA-dsDNA are nearly untilted and therefore unstacked [35]. Initial steps to analyze this will be taken in Sec. IV B, but as there are no experimental data concerning tilt elasticity, it is left out of the simple RecA-dsDNA model of Sec. IV A.

Two more points regarding RecA-dsDNA should be made. First, the functional biological relevance of RecA-dsDNA complexes is not established. For recombination to proceed at physiological pH, RecA must first form a filament around single-stranded DNA. The resulting RecA-ssDNA filament is capable of searching for sequence homology and invading a naked dsDNA molecule, and finally carrying out exchange of DNA strands between the ssDNA and dsDNA molecules. After strand exchange, the product double helix (one strand of which comes from the original ssDNA) tends to stay bound with RecA. The RecA-dsDNA complexes considered here may resemble this recombinant product complex.

Second, RecA-DNA binding is complicated by the fact that RecA can bind and hydrolyze ATP, an energy source [35]. The function of this ATP hydrolysis is not well understood: it has been variously proposed to regulate RecA-DNA filament disassembly, and to provide energy for DNA unwinding, homology search, and recombination [36]. The fact that RecA-DNA is able to steadily turn over ATP, may make binding models based on equilibrium statistical mechanics inappropriate. On the other hand, although ATP is required for RecA to bind two or three DNA strands, ATP hydrolysis is not necessary. RecA-DNA filaments can be prepared in the test tube with ATP- γS instead of ATP; ATP- γS can only be slowly hydrolyzed, thus making RecA-DNA binding plausibly described using equilibrium statistical mechanics.

A. Model for RecA-dsDNA binding

Suppose that $\phi(\xi)$ represents the occupation of site ξ along a DNA by RecA monomers; $\phi = 1$ denotes a site occupied by RecA, while $\phi = 0$ denotes bare DNA. The approach will be to consider $\phi(\xi)$ to be fixed, and then to calculate the DNA structure thus induced. This is appropriate since RecA binds very strongly to itself, forming filaments even in the absence of DNA and making RecA-DNA binding highly cooperative [34].

The binding of RecA to a DNA with freely fluctuating twist can be described by an addition to energy (1),

$$\frac{\Delta E}{k_B T} = \int_0^{L_0} d\xi [\mu_0 - \mu e^{-(u-u_0)^2/\delta^2} + \Gamma\Omega] \phi. \quad (22)$$

Here, μ is the “bare” RecA monomer–double-helix DNA binding free energy, in units of energy per length of unstretched DNA. The parameter u_0 is the DNA stretching energy

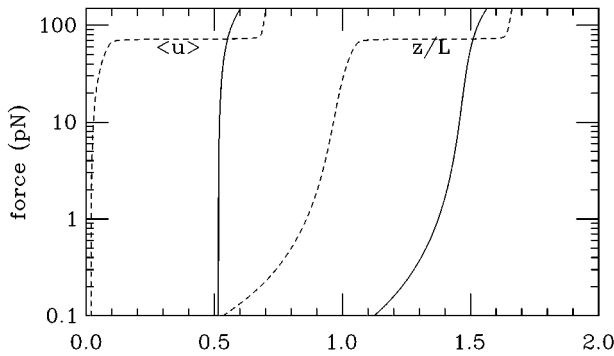


FIG. 8. Force-distance curves for RecA-DNA (solid) compared with bare DNA (dashed). The extension is in units of B -DNA length. RecA-DNA has no overstretching transition, since RecA binding already extends DNA to 1.5 times the B length. The left vertical curves show the longitudinal strain, which for RecA-DNA varies only from about 0.5 to 0.6 from forces of zero to 150 pN.

quired for RecA binding, and δ controls the width of the binding free energy for fluctuations of u away from u_0 . Below, $u_0 = 0.5$ (from the experimental observation that RecA-DNA filaments are 1.5 times the length of bare DNA) and $\delta = 0.15$ will be assumed. This potential makes RecA-DNA binding favorable only for u close to u_0 , while the torque Γ unwinds the double helix to the desired 18-bp repeat ($\Omega \approx -0.8$). The form of Eq. (22) was chosen for simplicity of calculation, while retaining the essential features of constraint of stretching and twisting. The constant μ_0 is the strain-independent part of the RecA-DNA binding free energy, which is, since one expects RecA to have little affinity for unstretched DNA, principally the concentration-dependent translational entropy lost when a RecA monomer binds DNA, plus RecA-RecA interactions (the latter could be appreciable given that RecA filaments can form in the absence of DNA). Including RecA-RecA interactions in μ_0 makes Eq. (22) the free energy of RecA-dsDNA relative to disassembled RecA monomers and bare DNA. Below, μ_0 is set to zero; a nonzero value simply will shift the model free energy of RecA-DNA by an amount proportional to the total number of RecAs bound.

No effect of RecA binding on the persistence length other than that implicit in Eq. (1) is considered here. Intuitively the persistence length of RecA-DNA should be greater than that of DNA, although no experimental data exist. With no other information available, the remaining elastic constants of RecA-DNA (w , γ_0 , q , g , and C_0) are assumed to be the same as for bare DNA.

The free energy may be computed using the Schrödinger-like equation approach of Sec. II; the only change is the addition of the potential terms of (22) to the free energy (1). The free energy $\lambda^{(\phi)} = (\ln Z)/L_0$, and the equilibrium distribution $\psi^{(\phi)}(\hat{\mathbf{t}}, u)$, may be computed for bare DNA ($\phi = 0$, the model studied in the previous sections) and for fully RecA-bound DNA ($\phi = 1$).

Figure 8 shows the force-distance behavior of bare DNA with no twist constraint (results of Sec. II, dashed lines), and RecA-DNA (solid lines), using parameters $\mu = 20 \text{ nm}^{-1}$ and $\Gamma = 40$ (each RecA monomer binds three base pairs, so /nm

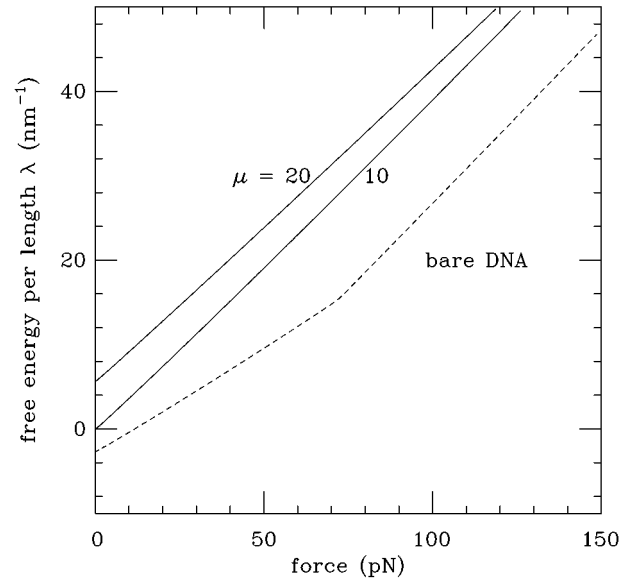


FIG. 9. Free energy (logarithm of partition function) of RecA-DNA (solid curves; the binding free energy per length is $\mu = 20$ and 10 nm^{-1} for the upper and lower curves, respectively) compared to that for bare DNA (dashed line). Solid lines do not include a constant contribution accounting for RecA-RecA interaction free energy per length, and RecA monomer entropy lost by binding (see text). The lack of an overstretching transition makes the RecA-DNA free energy nearly linear; bare DNA has a kink. At zero force, if RecA is bound, and its free energy must be above the dashed one; thus, even when force is applied, RecA binding will remain favorable.

units roughly correspond to /RecA). Both extensions are normalized to the B -DNA length L at zero force; the average stretching u indicates that the RecA-DNA filament is 1.50 times the B -DNA length at zero force and gives an average twist $\Omega = -0.76 \text{ rad/nm}$ corresponding to a 18-bp helix repeat. Bare DNA shows the familiar force plateau; in contrast, RecA-DNA has no force plateau, and behaves roughly like an *inextensible* wormlike chain of length $1.5L$. For forces $< 200 \text{ pN}$, it is not favorable to increase strain to the S state with $u \approx 0.6$ because the resultant free energy loss of roughly $\approx \mu k_B T / \text{nm} = 80 \text{ pN}$ cannot be overcome by the extension free energy $\approx 0.1f$. Note that since μ is doing the work of stretching the DNA it must be above some threshold value in order for DNA extension to occur at zero force; this threshold is approximately $\mu = 3 \text{ nm}^{-1}$. For larger μ , the force-distance behavior of RecA-DNA is essentially always that of Fig. 8.

Figure 9 shows the free energy λ for bare DNA (as per Sec. II), and RecA-DNA with $\mu = 10$ and 20 nm^{-1} . The bare DNA curve (dashed) has a kink at the B -DNA to S -DNA transition; RecA-DNA is nearly linear, with no kink. It should be recalled that the RecA-DNA curve has the unknown free energy offset μ_0 set to zero. The difference between the solid curves and the dashed curves at zero force may be regarded as the contribution of RecA-DNA interactions and the DNA elastic free energy to the net binding free energy; for the $\mu = 20$ curve, this is about $8k_B T / \text{nm}$, or about $8k_B T / (\text{RecA monomer})$. To this must be added μ_0 , the portion of the RecA-RecA interactions which are independent of

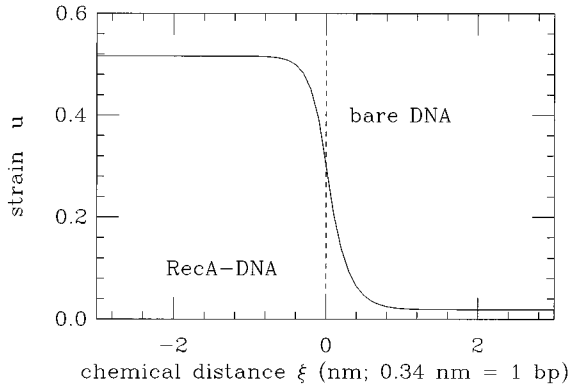


FIG. 10. Strain near a RecA-DNA–bare DNA “domain wall” (dashed line). In the RecA-DNA region the strain is near its asymptotic until it is less than 1 nm from the wall; the strain then rapidly decays to its *B*-DNA value. The length scale of the decay is the strain correlation length $\xi \approx (w/\gamma)^{1/2} \approx 0.2$ nm.

the presence of DNA strands. The solid curves of Fig. 9 can be freely shifted up and down by changes in μ_0 , which might be done experimentally by changing the RecA monomer concentration.

For RecA to be bound at zero force, the solid curves of Fig. 9 must be higher than the dashed one at zero force (equilibrium maximizes λ). The relative slopes of the curves of Fig. 9 therefore indicate that if RecA is bound at zero force, it will not be thermodynamically favorable for it to unbind at larger forces. On the other hand, if RecA is present at such low concentrations that it is not bound at zero force one might be able to observe it bind *as the DNA is stretched*; in Fig. 9 this corresponds to a solid curve shifted to be slightly below the dashed one at zero force so that there is a free energy crossing at an intermediate force. This tension-driven RecA-DNA association is exactly the opposite of the tension-driven *dissociation* expected for proteins which *reduce* free DNA contour (e.g., DNA-looping proteins such as the lac repressor, or the histone octamer) [15]. This effect might also be studied by reduction of μ (or Γ), possibly by using mutant RecA, using DNA-binding drugs or proteins to compete with RecA, or by use of high salt concentrations to

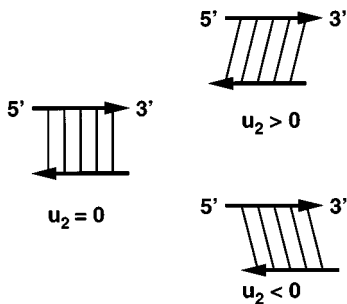


FIG. 11. A portion of DNA double helix with relaxed tilt ($u_2 = 0$) may be deformed by tilting the base pairs, leading to the sliding of one backbone past the other. Positive tilt ($u_2 > 0$) makes the 3' ends lead the 5' ends. Negative tilt is distinguishable from positive tilt.

reduce the electrostatic component of the DNA-RecA interactions (note that reducing μ from 20 to 10 essentially shifts the RecA-DNA free energy curve by a constant, Fig. 9).

Properties of the domain wall between regions where RecA is bound and bare DNA can also be investigated. Such domain walls can be observed in electron micrographs of RecA-DNA. The free energy of two distant domain walls is obtained by solving the Schrödinger equation given $\phi(\xi) = \Theta(\xi - L_0/2)$, assuming periodic boundary conditions connecting $\xi = 0$ to $\xi = L$. Since the Schrödinger equation is first order in s , the normalized ground states for $\phi = 0$ and $\phi = 1$ (all states have the normalization $\int d^2t du \psi^2 = 1$), can be used to write the partition function for the limit of large L_0 as

$$Z = \int d^2t' du' \int d^2t du \psi^{(0)}(\mathbf{t}', u') e^{\lambda^{(1)} L_0/2} \times \psi^{(0)}(\mathbf{t}, u) \psi^{(1)}(\mathbf{t}', u') e^{\lambda^{(0)} L_0/2} \psi^{(1)}(\mathbf{t}, u) = \langle 1|0 \rangle e^{\lambda^{(0)} L_0/2} \langle 0|1 \rangle e^{\lambda^{(1)} L_0/2}, \quad (23)$$

where the second line introduces “bra-ket” notation analogous to that used in quantum mechanics.

Subtracting the bulk part of the free energy [$\lambda^{(1)} - \lambda^{(0)}$] $L_0/2$ from $\ln Z$, the domain wall free energy D follows as the overlap of the equilibrium states for $\phi = 1$ and 0:

$$\frac{D}{k_B T} = -\ln |\langle 0|1 \rangle|. \quad (24)$$

This represents the contribution of the DNA degrees of freedom to the free energy cost of a single domain wall. For $\mu = 20 \text{ nm}^{-1}$, the domain wall free energy is $3.2 k_B T$. DNA deformation alone contributes $6.4 k_B T$ to the nucleation free energy for a RecA-DNA domain. The total nucleation free energy will include an additional contribution from RecA-RecA interactions not discussed here.

Finally, the average stretch along the bare DNA near this domain wall can be computed. This may be expressed using the complete set of eigenstates $\psi_i^{(\phi)}$ (or $|\phi, i\rangle$) and associated free energies $\lambda_i^{(\phi)}$, where $i = 0$ denotes equilibrium states:

$$\langle u(\xi) \rangle = \frac{\langle 1,0 | \sum_i |0,i\rangle e^{[\lambda_i^{(0)} - \lambda_0^{(0)}] \xi} \langle 0,i | u | 0,0 \rangle \langle 0,0 | 1,0 \rangle}{\langle 1,0 | 0,0 \rangle} \quad (25)$$

in the limit $L_0 \gg \xi$. The stretch in the RecA-bound region may be similarly expressed in terms of the $\phi = 1$ spectrum. Figure 10 shows the stretch distribution; the stretch “heals” over a distance ≈ 0.4 nm, roughly the spacing of successive base pairs, and close to the correlation length for Gaussian u fluctuations, $(w/\gamma)^{1/2} = 0.2$ nm.

B. Base-pair tilt elasticity

RecA-dsDNA has a constrained base-pair tilt. In order to account for the free energy cost of this constraint—ignored in Sec. IV A—the tilt elasticity of “bare” DNA must be considered. Given that the double helix is locally a ladderlike

structure with the base pairs forming the rungs, tilt is simply defined in terms of the angle between the centerline of the base pairs, and the local chain direction $\hat{\mathbf{t}}(\xi)$. The tangent of the change of this angle from its equilibrium will be considered as a tilt strain variable $u_2(\xi)$. The excess tilt angle will be considered positive when the two 3' ends of a local portion of double helix protrude beyond the two 5' ends (Fig. 11).

Since the two backbones are oppositely directed (Fig. 11), positive and negative u_2 are distinct. Therefore, both $u_2 u$ and $u_2 \Omega$ are permitted as terms in the elastic energy: both tilt-stretch and tilt-twist couplings exist. This matches the notion that in order for base stacking interactions to be undisturbed as the double helix is untwisted or stretched, the base-pair tilt must increase.

So, a more detailed elastic model than that of Eq. (1), which includes u_2 as well as u and Ω , is

$$\frac{E}{k_B T} = \int_0^{L_0} \left\{ \frac{C_1}{2} \Omega^2 + \frac{\gamma_1}{2} u^2 + \frac{w}{2} \left(\frac{\partial u}{\partial \xi} \right)^2 + g_1 u \Omega + \frac{\gamma_2}{2} u_2^2 - \gamma_{12} u u_2 + g_2 u_2 \Omega - h u_2 + \dots \right\}, \quad (26)$$

where only the terms differing from those of Eq. (1) are tabulated. The elastic constants γ_1 , γ_2 , and γ_{12} should be roughly comparable in magnitude to $\gamma_0 \approx 300 \text{ nm}^{-1}$. Similarly, g_1 and g_2 should be on the order of $g \approx 30$. Stability requires that the interaction matrix coupling u , u_2 , and Ω be positive definite. Finally a ‘‘tilt field’’ h is included; $h=0$ for bare DNA as considered in Secs. II and III, while a non-zero value allows tilt to be constrained.

The tilt fluctuations can be integrated out to leave an effective free energy which depends only on u and Ω , and is of the form of Eq. (1), with elastic constants $C_0 = C_1 - g_2^2/\gamma_2$, $\gamma_0 = \gamma_1 - \gamma_{12}^2/\gamma_2$, and $g = g_1 + g_2 \gamma_{12}/\gamma_2$. The tilt fluctuations soften the twist and stretch elasticity in the same way that twist fluctuations softened the stretch modulus of Eq. (2). Nonzero h adds torque and tension contributions (h/γ_2)[$g_2 \Omega - \gamma_{12} u$] to the effective free energy per length, after tilt fluctuations are integrated out. Finally, the expectation value of the tilt is

$$\langle u_2(\xi) \rangle = [\gamma_{12} u(\xi) - g_2 \Omega(\xi) + h] / \gamma_2 \quad (27)$$

analogous to Eq. (3) of Sec. II. The signs of γ_{12} and g_2 have been chosen so that for positive values, the double-helix tilt rises with stretching or untwisting.

So, integration of harmonic tilt fluctuations reduces Eq. (26) to Eq. (1). Unfortunately, no experimental data exist which indicate what the many elastic constants of Eq. (26) should be. The crucial coupling is γ_{12} , which is likely large (i.e., comparable to γ_1 and γ_2) as simulations [6] indicate that base-pair tilt u_2 is roughly as large as helix stretching u for $u \approx 0.1$, where there is very little helix untwisting. Perhaps the elastic constants of Eq. (26) could be extracted from numerical simulations, or better, from atomic force microscopy experiments on oligonucleotides with *both* strands an-

chored at both ends. Alternately, if base-pair tilt could be measured during stretching of a long DNA, γ_{12} could be estimated using Eq. (27).

Even if the linear tilt elasticity was understood, a further problem is that for application to RecA-dsDNA, nonlinear tilt elasticity should be considered, since the untilted and stretched DNA in RecA filaments is unstacked. Passage of DNA to this state certainly involves a large free energy barrier associated with exposure of the hydrophobic bases.

V. RELAXATION DYNAMICS OF AN OVERSTRETCHED DNA

Stress on a DNA perturbs its twist. For strong overstretching ($L/L_0 \approx 1.6$), the double helix is 20% underwound in the model of Sec. II. Numerical simulations [25] suggest that even larger untwistings may result from overstretching. How will a stored twist affect DNA relaxation when stress is quickly released? Without any initial twisting, a DNA (or other polymer) relaxes from a fully stretched state in a time $\tau_{\text{flower}} \approx L^2 A \eta / k_B T$, where η is the solvent (aqueous buffer) viscosity. The chain relaxes from its ends by the formation of random-coil ‘‘flowers’’ at the ends of a stretched intervening ‘‘stem’’ [37,16]. For a 10- μm DNA, and taking $\eta = 0.01$ poise, $\tau_{\text{flower}} \approx 1$ s.

Twist relaxation is opposed by rotational drag along the length of the molecule, and occurs on a time on the order of $\tau_{\text{twist}} \approx L^2 d^2 \eta / (k_B T C_0)$, where $d \approx 2$ nm is the double helix hydrodynamic radius [38]. This is the time required for the twist to wind out through the molecule ends, and scales similarly to τ_{stretch} with L , although with a much smaller prefactor. For a 10- μm DNA, $\tau_{\text{twist}} \approx 10^{-3}$ s.

For overstretched DNA, there is a third relaxation time associated with retraction of the stretching. Retraction is driven by γ_0 (this will be shown in detail below), and is opposed by hydrodynamic drag along the length of the chain. Balance of these opposing forces leads to a retraction time of $\tau_{\text{retract}} \approx \eta L^2 / (k_B T \gamma_0)$. For our same 10- μm DNA, $\tau_{\text{retract}} \approx 10^{-4}$ s. Note that all of these relaxation times scale in the same way with L (ignoring long-ranged hydrodynamic flow effects) and thus these time scales will be separated by similar factors for any L .

The separation of these time scales suggests an interesting relaxation dynamics for a long overstretched molecule. First, in a time τ_{retract} , the contour length of the molecule will be restored to near L . Next, over a time τ_{twist} , the twist on the molecule will relax, and then finally the chain ends will flower and the molecule will regain a relaxed random coil configuration over a time τ_{flower} .

Now consider the relaxing molecule during times $\tau_{\text{retract}} < t < \tau_{\text{twist}}$. According to the above, the stretch $u(s)$ will have relaxed, but the twist $\Omega(s)$ will be far from relaxed. A region in the interior of the molecule will be under twist strain, and of course cannot sense whether that twist strain is supported by a static torque, or by hydrodynamic friction. Therefore, for sufficiently large Ω the molecule should become unstable to writhing (coiling). Below it will be shown that there is indeed such an instability, for regions of the chain where $(C\Omega + gu)^2 > 4A(\gamma u + g\Omega)$. This instability is really just the static writhe instability of Eq. (20), but here it will be recovered without any reference to fixed linkage

number of the double helix, as is appropriate for the relaxing open chain; only force and torque balance between successive chain segments and the surrounding aqueous buffer will be considered.

A. Dynamical model

The model to be considered is entirely dissipative and local, where forces and torques on a chain segment are determined by the velocities and angular velocities of only that segment. In polymer nomenclature, these are ‘‘Rouse’’ dynamics, which ignore the long-ranged hydrodynamic interactions between distant segments. First and foremost, this approximation is important since it makes the calculations which follow tractable; a similar approximation is commonly used in models of DNA twisting dynamics [38], and was recently used by Kamien in his study of linkage density dynamics [17].

The unfortunate fact is that the interactions induced between distant segments by the fluid flow are important for quantitative study of the bending dynamics of even highly stretched chains in free solution. For example, Zimm [39] estimated that the friction on DNA's of $L \approx 40\mu$ stretched by flow is overestimated by about 40% if hydrodynamic interactions are neglected. So, the results of this section can be regarded as only a qualitative guide.

As in the preceding sections, a DNA molecule is described by the chain contour $\mathbf{r}(\xi)$, and an internal twist degree of freedom. The twist degrees of freedom may be described by a unit vector director $\hat{\mathbf{e}}(\xi)$, constrained to be orthogonal to the chain tangent (unit vector) $\hat{\mathbf{t}} \equiv d\mathbf{r}/d\xi/|d\mathbf{r}/d\xi|$. Unstressed DNA is taken to have a perfectly straight contour, with $|d\mathbf{r}/d\xi|=1$, and constant $\hat{\mathbf{e}}$ (the equilibrium B-DNA twist is removed). Twist strain is then simply the circulation of $\hat{\mathbf{e}}$ around $\hat{\mathbf{t}}$, $\Omega \equiv \hat{\mathbf{t}} \times \hat{\mathbf{e}} \cdot d\hat{\mathbf{e}}/d\xi$ [7].

The DNA elastic energy to be studied is a truncated version of Eq. (1),

$$\frac{E}{k_B T} = \int_0^{L_0} d\xi \left[\frac{A}{2} \left(\frac{d^2 \mathbf{r}}{d\xi} \right)^2 + \frac{C_0}{2} \Omega^2 + \frac{\gamma_0}{2} u^2 + g u \Omega \right], \quad (28)$$

where, as before, the longitudinal strain is $u = |d\mathbf{r}/d\xi| - 1$. With regard to Eq. (1), a slightly different curvature energy is used, and the nonlinear potential $V(u)$ and the force term have both been dropped.

Rouse dynamics of the backbone $\mathbf{r}(\xi)$ are determined by balance of driving and dissipative forces:

$$\frac{\partial \mathbf{r}}{\partial t} = - \frac{1}{\zeta} \frac{\delta E}{\delta \mathbf{r}}. \quad (29)$$

The friction constant ζ is solvent viscosity, times an order-unity factor.

The dynamics for $\hat{\mathbf{e}}(\xi)$ are determined by a balance of driving and dissipative torques [40]:

$$\frac{\partial \hat{\mathbf{e}}}{\partial t} = - \frac{1}{\zeta_R} \left(\hat{\mathbf{e}} \times \frac{\delta E}{\delta \hat{\mathbf{e}}} \right) \times \hat{\mathbf{e}}. \quad (30)$$

Although it appears that this is an equation for two angular degrees of freedom, projecting out motion which violates the

constraint $\hat{\mathbf{e}} \cdot \hat{\mathbf{t}} = 0$ reduces it to a single ‘‘twist’’ equation, in accord with the static description of Sec. II. For the situations to be discussed here, the twist dynamics will be mainly circulation of $\hat{\mathbf{e}}$ around $\hat{\mathbf{t}}$. Thus ζ_R will be considered to be solvent viscosity times the square of DNA hydrodynamic radius d , times a dimensionless order-unity factor (in general, angular velocities in the directions of $\hat{\mathbf{t}}$ and $\hat{\mathbf{t}} \times \hat{\mathbf{e}}$ should be multiplied by rotary frictions differing by a geometrical factor).

Equations (29) and (30), in combination with Eq. (28) and the constraint $\hat{\mathbf{e}} \cdot \hat{\mathbf{t}} = 0$, define relaxational dynamics. Given initial conditions and suitable boundary conditions (no forces, curvatures, or twist torques on the ends), the dynamics can be integrated. For an initially stretched and twisted molecule, the initial condition is that of uniform extension and twist strains, or $\mathbf{r}(\xi) = (1 + u_0)\xi \hat{\mathbf{z}}$ and $\hat{\mathbf{e}}(\xi) = \hat{\mathbf{x}} \cos(\theta) + \hat{\mathbf{y}} \sin(\theta)$, where $\theta = \Omega_0 \xi$. For the special case where the molecule is not under initial torque, the initial (under)twist is $\Omega_0 = -g u_0 / C_0$; this state would follow from equilibration against a force $f = k_B T \gamma u_0$ with no constraint on twist.

The relaxation dynamics after release of the force may be described in terms of longitudinal (z) and transverse (xy) displacements of the contour and director variables:

$$\mathbf{r} = (\xi + r_{\parallel}) \hat{\mathbf{z}} + \hat{\mathbf{r}}_{\perp}, \quad (31)$$

$$\hat{\mathbf{e}} = \hat{\mathbf{z}} e_{\parallel} + (1 - e_{\parallel}^2)^{1/2} (\hat{\mathbf{x}} \cos \theta + \hat{\mathbf{y}} \sin \theta).$$

For a nearly straight initially stretched and twisted chain, the variables e_{\parallel} and $\hat{\mathbf{r}}_{\perp}$ are zero, while the stretch and twist strains, $dr_{\parallel}/d\xi$ and $d\theta/d\xi$, are constant. In what follows, contributions to the energy quadratic in \mathbf{r}_{\perp} , r_{\parallel} , and θ will be kept, to obtain a linearized dynamics. The stretch and twist strains will turn out to act as local parameters controlling writhing, which will appear as an instability of \mathbf{r}_{\perp} . So, terms linear in one of $dr_{\parallel}/d\xi$ and $d\theta/d\xi$, and in addition quadratic in \mathbf{r}_{\perp} , will also be kept.

First, the constraint $\hat{\mathbf{e}} \cdot \hat{\mathbf{t}} = 0$ must be imposed; this is conveniently done by elimination of e_{\parallel} , which to linear order in \mathbf{r}_{\perp} is

$$e_{\parallel} = - \frac{dx_{\perp}}{d\xi} \cos \theta - \frac{dy_{\perp}}{d\xi} \sin \theta. \quad (32)$$

Next the curvature squared, longitudinal strain, and twist strain may be expressed as

$$\left(\frac{d^2 \mathbf{r}}{d\xi^2} \right)^2 = \left(\frac{d^2 r_{\parallel}}{d\xi} \right)^2 + \left(\frac{d^2 \mathbf{r}_{\perp}}{d\xi} \right)^2, \quad (33)$$

$$\left| \frac{d\mathbf{r}}{d\xi} \right| = 1 + \frac{dr_{\parallel}}{d\xi} + \frac{1}{2} \left(\frac{d\mathbf{r}_{\perp}}{d\xi} \right)^2 + \text{h.o.t.},$$

$$\hat{\mathbf{t}} \times \hat{\mathbf{e}} \cdot \frac{d\hat{\mathbf{e}}}{d\xi} = \left[1 + \frac{dr_{\parallel}}{d\xi} + \left(\frac{d\mathbf{r}_{\perp}}{d\xi} \right)^2 \right] \frac{d\theta}{d\xi} + \frac{1}{2} \hat{\mathbf{z}} \cdot \frac{d^2 \mathbf{r}_{\perp}}{d\xi^2} \times d\mathbf{r}_{\perp} + \text{h.o.t.} \quad (34)$$

Terms of higher than linear order (h.o.t.) in r_{\parallel} and higher than quadratic order in \mathbf{r}_{\perp} have been dropped. Also, in the

final twist expression, contributions containing $\cos \theta$ and $\sin \theta$ have been averaged over $0 < \theta < 2\pi$. The energy follows as

$$\begin{aligned} \frac{E}{k_B T} = & \int_0^{L_0} d\xi \left\{ \frac{\gamma_0}{2} \left(\frac{dr_{\parallel}}{d\xi} \right)^2 + \frac{A}{2} \left(\frac{d^2 r_{\parallel}}{d\xi^2} \right)^2 \right. \\ & + \frac{C_0}{2} \left(\frac{d\theta}{d\xi} \right)^2 + g \frac{d\theta}{d\xi} \frac{dr_{\parallel}}{d\xi} + \frac{A}{2} \left(\frac{d^2 \hat{\mathbf{r}}_{\perp}}{d\xi} \right)^2 \\ & + \frac{1}{2} \left[\gamma_0 \frac{dr_{\parallel}}{d\xi} + g \frac{d\theta}{d\xi} \right] \left(\frac{d\mathbf{r}_{\perp}}{d\xi} \right)^2 + \frac{1}{2} \\ & \left. \times \left[C_0 \frac{d\theta}{d\xi} + g \frac{dr_{\parallel}}{d\xi} \right] \hat{\mathbf{z}} \cdot \frac{d^2 \mathbf{r}_{\perp}}{d\xi^2} \times \frac{d\mathbf{r}_{\perp}}{d\xi} + \text{h.o.t.} \right\}. \quad (35) \end{aligned}$$

The first four terms of (35) generate coupled, linear dissipative dynamics for the stretch and twist degrees of freedom. In terms of Fourier transforms $\tilde{r}_{\parallel}(q)$ and $\tilde{\theta}(q)$, the dynamics are

$$\begin{aligned} \zeta \frac{\partial \tilde{r}_{\parallel}}{\partial t} = & -q^2 [(\gamma_0 + Aq^2)\tilde{r}_{\parallel} - g\tilde{\theta}], \\ \zeta_R \frac{\partial \tilde{\theta}}{\partial t} = & -q^2 [C_0 \tilde{\theta} + g\tilde{r}_{\parallel}]. \quad (36) \end{aligned}$$

For the experimentally relevant case where $g^2 \ll C_0 \gamma_0$ and $\gamma_0 \gg C_0/d^2$, the two molecule-long modes ($q = \pi L/4$) relax on two separated timescales. The shorter of the two is the retraction time characterizing relaxation of r_{\parallel} , $\tau_{\text{retract}} \approx \eta L^2 / (k_B T \gamma_0)$. The longer is the molecule unwinding time [38] $\tau_{\text{twist}} \approx \eta d^2 L^2 / (k_B T C_0)$. The eigenmodes for these decays are spread over the entire molecule, so the strains will spatially slowly vary.

The last three terms of Eq. (35) generate the equation of motion for \mathbf{r}_{\perp} , where in the cubic terms of Eq. (35) the strains $u \equiv dr_{\parallel}/d\xi$ and $\Omega \equiv d\theta/d\xi$ are considered constant:

$$\zeta \frac{\partial \tilde{\mathbf{r}}_{\perp}}{\partial t} = -q^2 (Aq^2 + \gamma_0 u + g\Omega + [C_0 \Omega + gu] i q \hat{\mathbf{z}} \times) \tilde{\mathbf{r}}_{\perp}. \quad (37)$$

The strains u and Ω control the stability of \mathbf{r}_{\perp} : large u stabilizes while large Ω , acting in the chiral term which couples the x and y components of \mathbf{r}_{\perp} , destabilizes. Eq. (37) may be diagonalized to obtain two decay rates

$$\lambda_{\pm} = \frac{k_B T q^2}{\zeta} (Aq^2 \pm [C_0 \Omega + gu] q + \gamma_0 u + g\Omega). \quad (38)$$

In local twist-stretch equilibrium $\Omega = -gu/C_0$, all the modes are stable ($\lambda_{\pm} > 0$ for $q \neq 0$); there is no tendency toward writhing. However, as $C_0 \Omega + gu$ is increased in mag-

nitude, there will be a slowing of one mode, and a stiffening of the other. The slower rate is λ_+ , and when the point $(C_0 \Omega + gu)^2 = 4A(\gamma_0 u + g\Omega)$, a nontrivial zero mode $\lambda_+(q^*) = 0$ appears at $q^* = \pm C_0 \Omega / A$.

So, for $(C_0 \Omega + gu)^2 > 4A(\gamma_0 u + g\Omega)$, \mathbf{r}_{\perp} is unstable to developing solenoidal writhe of wavelength $2\pi A / (C_0 \Omega)$. This is just the dynamic version of the static writhing instability discussed in Sec. III. Since the tension in the chain is $f = k_B T (\gamma_0 u + g\Omega)$ [see Eq. (15)], and twist strain corresponds to linkage $\sigma = \Omega / \omega_0$, the dynamic instability corresponds to the static one of, e.g., Eq. (20), $(C\omega_0 \sigma + gf / [k_B T \gamma_0])^2 < 4fA / k_B T$.

If an overstretched DNA is released, the stretching will relax after time t a distance $\sim (L^2 t / \tau_{\text{retract}})^{1/2}$ from the free end; at the same time, the twist relaxation will penetrate a distance $\sim (L^2 t / \tau_{\text{twist}})^{1/2}$, which is shorter by a factor $(C/d^2 \gamma)^{1/2} \approx 0.25$. The writhe instability will therefore ‘‘sweep’’ into a long chain from its free end.

The inverse of the typical instability amplification rate (38) indicates that $d\mathbf{r}_{\perp}/d\xi$ will become of order unity (i.e., the chain will become appreciably bent) at a time of $\tau_{\text{writhe}} \approx \zeta A^3 / (k_B T C^4 \Omega_0^4)$; this is a time on the order of the persistence length reorientation time $\zeta A^3 / k_B T \approx 30 \mu\text{s}$, and is shorter than, e.g., τ_{retract} , suggesting that appreciable writhing will begin near the free end of a long chain even before retraction is complete. What happens after the initial instability is difficult to study analytically, but, qualitatively, it is clear that the instability will occur inhomogeneously along the chain thanks to the differing rates for retraction, untwisting, and writhing.

B. Plectonemic supercoiling

Above, it was shown that the chain can writhe if it is sufficiently twisted before its release. For sufficiently long chains, it is plausible that plectonemic supercoils (wrapping of DNA around itself, as a twisted telephone cord does) will form to further relax the twist [10]. Plectoneme formation requires substantial transfer of chain contour; for a transfer velocity v , the associated drag force is $\approx \eta L v$. This drag is overcome by the driving force due to the free energy difference per length Δ of the twisted DNA and supercoiled DNA, so the velocity with which a plectonemic region can form is $v \approx \Delta / (\eta L)$. Since the stretching has been predominantly relaxed before writhing can occur, Δ will be made up of the twisting energy (which can be saved by formation of a tight plectoneme [27]) $k_B T C_0 \Omega^2 / 2$. Taking $C_0 = 75 \text{ nm}$ and $\Omega \approx -0.25$ gives $\Delta \approx 2k_B T / \text{nm}$.

The time window over which plectoneme formation can operate is τ_{twist} . So the length of molecule which can supercoil is $\ell = v \tau_{\text{twist}} = (\Delta d^2 / k_B T C) L$. If Δ is $2k_B T / \text{nm}$ then $\Delta d^2 / (k_B T C_0) \approx 0.10$, and ℓ will be comparable to L . An overstretched, twisted DNA thus has time to develop supercoiled domains along an appreciable fraction of its length as it relaxes. The main unanswered question is how plectonemic regions nucleate; Brownian dynamics studies of long chains could illuminate this.

The relaxation processes outlined in this section require twist rigidity along the length of the molecule. DNA which has had one strand ‘‘nicked’’ at many places (less than a persistence length A between nicks) along its length should

be able to relax from an overstretched state by “internal” unwinding; no supercoiling should occur in the interior region of such a chain during its relaxation. Finally, if the nicks are spaced a distance $\ell \gg A$, the twist relaxation of the entire chain will occur over a τ_{twist} characteristic of a chain of length ℓ .

C. “Speedometer cable” twisting of DNA

A related biophysical problem is the conformation of a DNA with a torque applied to one end, and the other end free. Levinthal and Crane [41] argued that, to minimize dissipation, the double helix should simply rotate around its axis, like a “speedometer cable.” Although those authors had DNA replication in mind, the most likely biological realization of this occurs during transcription of linear DNA. Since RNA polymerase “tracks” the helical structure of DNA, a torque is applied to the double helix as transcription proceeds. This torque is $\approx 10k_B T$, since ≈ 1.7 NTP’s are hydrolyzed per radian of double helix transcribed. This level of torque is sufficient to generate DNA supercoiling on circular plasmids [42].

A similar twisting of a dsDNA was recently done [43] by pulling its two strands apart. The twists removed by “unzipping” were forced into the remaining double helix, forcing it to spin around its axis. Given that ≈ 10 pN were needed to unzip two DNA strands [43], the torque on the double helix was $\approx 10 \text{ pN} \times 2 \text{ nm} \approx 5k_B T$, comparable to that estimated above for transcription.

Ignoring writhing for the moment, the twist due to this level of torque ($10k_B T$) follows from the DNA twist energy as $|\Omega| \approx 10/C_0 \approx 0.13 \text{ nm}^{-1}$. In terms of a linkage change for an unwritted chain, this corresponds to $|\sigma| = 0.07$; static linkages of this magnitude are sufficient to change DNA secondary structure. Of course, this Ω is sufficient to cause writhing by the mechanism of Sec. V, for DNA tensions of up to $0.5k_B T/\text{nm} \approx 2 \text{ pN}$. The extent and amplitude of writhing will in this case be controlled by local balance of driving and dissipative torques; this and the effect of thermal and intrinsic DNA bending, remains to be studied in detail.

A high level of twisting will only be present near the rotated end of the chain; going down the chain, twisting and torque will decay away. For an unwritted chain with one steadily rotated end, the torque will vary roughly linearly along the chain contour, dropping to zero at the free end [44]. Finite-duration twist “packets” (as generated by RNA polymerase or gyrase activity) will propagate and spread down the chain in a manner reminiscent of diffusion [see Eq. (36)] with a twist density diffusion constant of $D_{\text{tw}} = k_B T C_0 / (\eta d^2) = 7.5 \times 10^{-4} \text{ cm}^2/\text{s}$. Even without consideration of writhing, these two effects already limit the distance from a transcription or gyrase site that strong twisting, and therefore DNA secondary structure change, can occur.

As an example of the latter limiting effect, consider a gyrase which takes out one turn at one end of a DNA. For linkage concentrated entirely in twist, $\sigma = -0.02$ is sufficient to alter DNA secondary structure; the twist strain generated by a single turn will dissipate to this level after it has spread out over 50 DNA turns ($= 500 \text{ bp} = 150 \text{ nm}$). The time required for this spreading is $(150 \text{ nm})^2 / D_{\text{tw}} \approx 3 \times 10^{-7} \text{ s}$, small compared to the $\approx 1 \text{ s}$ recovery time of gyrase. This

range of 500 bp for modification of DNA secondary structure by insertion of a single twist is in rough agreement with the result of a recent experimental observation of a range effect for modification of DNA secondary structure by gyrase and RNA polymerase activity [45].

VI. CONCLUSIONS

The elasticity of *B*-DNA is well described by the bending fluctuations of an inextensible wormlike chain for applied tensions below 10 pN. However, for larger tensions DNA’s secondary structure—the double helix—starts to stretch. Symmetry considerations indicate that *B*-DNA should untwist as it stretches [8,10]; experimental data in the small deformation regime [9] have allowed the linear coupling of stretch to twist to be determined [8,12]. Similarly, internal tilting of the base pairs in the double helix is coupled to both stretching and twisting at linear order in elastic theory.

For very large forces $\approx 70 \text{ pN}$, a new “*S*-DNA” state is obtained, 1.6 times longer than the *B*-form [5]; the experimentally observed force “plateau” at the *B*-DNA to *S*-DNA transition without torsional constraint indicates that the transition is highly cooperative [4]. Fitting the plateau shape to a simple model of the transition indicates that the correlation length for unperturbed *B*-DNA strain fluctuations is $\approx 0.2 \text{ nm}$, or at the scale of successive base pairs, and that typical microscopic strain fluctuations have an amplitude ≈ 0.1 . This analysis suggests a microscopic picture of unperturbed DNA which has appreciable fluctuations on top of a well-defined *B*-DNA state. Since DNA must often be untwisted and otherwise distorted to perform its biological functions, it is gratifying to see that it is not held too strongly to some canonical “*B*-DNA structure:” thermal fluctuations provide a range of local double helix conformations: particular fluctuations can be “grabbed” by DNA-binding proteins.

Holding the twist fixed during overstretching [11] provides a second way to measure the coupling of twist to stretch [10], and leads to an estimate for the linear twist-stretch coupling in agreement with that obtained for small strains. Combining the linear twist-stretch coupling with the nonlinearities which define the *S*-DNA state leads to a prediction that *S*-DNA is underwound by about 20% to have a helix repeat of 12.5 bp. Even higher extension may lead to the fully untwisted “ribbon” structure observed in simulations [4,25,6]. This extreme untwisting could be added to the present model by addition of couplings of twist to quadratic and higher powers of stretching strain. However, experiments to determine the twist of overstretched DNA, and to study the relation of *S*-DNA to melted DNA (Fig. 7) are needed to guide such additions.

A model for RecA-dsDNA has also been presented, in which a stretch- and twist-dependent binding potential provides the driving free energy for the observed overstretching and undertwisting. The main predictions of this model are that there should be no transition to *S*-DNA (since the DNA is “prestretched”) or tension-driven dissociation of RecA even at very high forces. Instead it may be possible to observe tension-driven association of RecA at, e.g., sufficiently low RecA monomer concentrations.

Finally, a simple dynamical model for relaxation of overstretched and undertwisted DNA has been discussed. Thanks

to the rather large stretch modulus, the stretch relaxes quickly, compared to the twist. As a result, the DNA can find itself in a state where it is unstable to writhing. Here, only the onset of writhing was studied in detail; the possibility that the chain will plectonemically supercoil remains to be carefully analyzed. However, a simple scaling argument suggests that at least part of the chain should become tightly supercoiled before the twist leaks out the free end. Simulations including self-avoidance, long-ranged hydrodynamic interaction, and thermal fluctuation effects are needed to

study relaxation of twisted DNA, and the behavior of twist-driven DNA.

ACKNOWLEDGMENTS

The author thanks K. Adzuma, R. Kamien, P. Nelson, G. V. Shivashankar, E. Siggia, and T. Witten for many helpful discussions of these problems, and D. Bensimon, D. Chatenay, P. Cluzel, V. Croquette, and T. Strick for discussions and for communicating their experimental data.

-
- [1] S. B. Smith, L. Finzi, and C. Bustamante, *Science* **258**, 1122 (1992).
- [2] T. T. Perkins, S. R. Quake, D. E. Smith, and S. Chu, *Science* **264**, 822 (1994); T. T. Perkins, D. E. Smith, R. G. Larson, and S. Chu, *ibid.* **268**, 83 (1995).
- [3] C. Bustamante, J. F. Marko, S. B. Smith, and E. D. Siggia, *Science* **265**, 1599 (1994); A. Vologodskii, *Macromolecules* **27**, 5623 (1994).
- [4] P. Cluzel, A. Lebrun, C. Heller, R. Lavery, J.-L. Viovy, D. Chatenay, and F. Caron, *Science* **271**, 792 (1996).
- [5] S. B. Smith, Y. Cui, and C. Bustamante, *Science* **271**, 795 (1996); S. B. Smith, Y. Cui, A. C. Hausrath, and C. Bustamante, *Biophys. J.* **68**, A250 (1995).
- [6] A. Lebrun and R. Lavery, *Nucl. Acid. Res.* **24**, 2260 (1996).
- [7] J. F. Marko and E. D. Siggia, *Macromolecules* **28**, 8759 (1995).
- [8] R. D. Kamien, T. C. Lubensky, P. Nelson, and C. S. O'Hern, *Europhys. Lett.* **38**, 237 (1997); C. S. O'Hern, R. D. Kamien, T. C. Lubensky, and P. Nelson, *Eur. Phys. J. B* **1**, 95 (1998).
- [9] T. R. Strick, J.-F. Allemand, D. Bensimon, A. Bensimon, and V. Croquette, *Science* **271**, 1835 (1996).
- [10] J. F. Marko, *Europhys. Lett.* **38**, 183 (1997).
- [11] P. Cluzel, Ph.D. thesis, University de Paris VI, 1996 (unpublished).
- [12] D. Moroz and P. Nelson, *Proc. Natl. Acad. Sci. USA* (to be published).
- [13] C. Bouchiat and M. Mezard (unpublished).
- [14] A. Stasiak and E. Di Capua, *Nature (London)* **299**, 185 (1982); E. H. Egelman and A. Stasiak, *J. Mol. Biol.* **191**, 677 (1986).
- [15] J. F. Marko and E. D. Siggia, *Biophys. J.* **73**, 2173 (1997).
- [16] F. Brochard-Wyart, *Europhys. Lett.* **30**, 387 (1995); **23**, 105 (1993).
- [17] R. D. Kamien, *Eur. Phys. J. B* **1**, 1 (1998).
- [18] D. M. Crothers, J. Drak, J. D. Kahn, and S. D. Levene, *Meth. Enzymology* **212**, 3 (1992).
- [19] K. V. Klenin, A. V. Vologodskii, V. V. Anshelevich, V. Y. Klisko, A. M. Dykhne, and M. D. Frank-Kamenetskii, *J. Biomol. Struct. Dyn.* **6**, 707 (1989).
- [20] J. F. Marko and E. D. Siggia, *Macromolecules* **27**, 981 (1994).
- [21] N. Saito, K. Takahashi, and Y. Yunoki, *J. Phys. Soc. Jpn.* **22**, 219 (1967).
- [22] T. Odijk, *Macromolecules* **28**, 7016 (1995).
- [23] M. D. Wang, H. Yin, R. Landick, J. Gelles, and S. M. Block, *Biophys. J.* **72**, 1335 (1997).
- [24] D. Bensimon, A. J. Simon, V. Croquette, and A. Bensimon, *Phys. Rev. Lett.* **74**, 4754 (1994); *Science* **265**, 2096 (1995).
- [25] M. W. Konrad and J. I. Bolonick, *J. Am. Chem. Soc.* **118**, 10989 (1996).
- [26] A. Noy, D. V. Vezenov, J. F. Kayyem, T. J. Meade, and C. M. Lieber, *Chem. Biol.* **4**, 519 (1997).
- [27] J. F. Marko and E. D. Siggia, *Science* **265**, 506 (1994); *Phys. Rev. E* **52**, 2912 (1995); J. F. Marko, *ibid.* **55**, 1758 (1997).
- [28] A. V. Vologodskii and J. F. Marko, *Biophys. J.* **73**, 123 (1997).
- [29] B. Fain, S. Ostlund, and J. Rudnick (unpublished).
- [30] F. B. Fuller, *Proc. Natl. Acad. Sci. USA* **68**, 815 (1971).
- [31] A. E. H. Love, *Mathematical Treatise on the Theory of Elasticity* (Dover, New York, 1941), Sec. 269.
- [32] J. F. Marko, *Phys. Rev. E* **55**, 1758 (1997).
- [33] P. Baumann, F. E. Benson, and S. C. West, *Cell* **87**, 757 (1996).
- [34] M. Takahashi, *J. Biol. Chem.* **264**, 288 (1989).
- [35] M. Takahashi and B. Norden, *Adv. Biophys.* **30**, 1 (1994).
- [36] M. M. Cox, *Trends Biochem. Sci.* **19**, 217 (1994).
- [37] P.-G. de Gennes, *J. Chim. Phys. Phys.-Chim. Biol.* **87**, 962 (1967).
- [38] M. D. Barkley and B. H. Zimm, *J. Chem. Phys.* **70**, 2991 (1979).
- [39] B. H. Zimm (unpublished).
- [40] M. Doi and S. F. Edwards, *Theory of Polymer Dynamics* (Cambridge University Press, Cambridge, 1985), Sec. 8.2.
- [41] C. Levinthal and H. R. Crane, *Proc. Natl. Acad. Sci. USA* **42**, 436 (1956).
- [42] L. F. Liu and J. C. Wang, *Proc. Natl. Acad. Sci. USA* **84**, 7024 (1987); H.-Y. Wu, S. H. Shuy, J. C. Wang, and L. F. Liu, *Cell* **53**, 433 (1988); Y.-P. Tsao, H.-Y. Wu, and L. F. Liu, *ibid.* **56**, 111 (1989).
- [43] B. Essevaz-Roulet, U. Bockelmann, and F. Heslot, *Proc. Natl. Acad. Sci. USA* **94**, 11935 (1997).
- [44] A. V. Vologodskii (private communication).
- [45] L. Rothman-Denes (unpublished).